information about cell behavior in tissues consisting of homogeneous cell types, cultured cells, and cancer tissues of monoclonal origin.[12,13] In the case of neuronal tissues, particularly those of patients with neurological diseases, however, the complexity of tissues containing multiple lineages of cells, such as neurons, glial cells, and vascular tissues, places limitations on the use of DNA microarray technology. In the lesions of ALS spinal cords, there are reduced numbers of motor neurons with glial cell proliferation, making it difficult to examine motor neuron–specific gene expression.

Laser-captured microdissection (LCM) has been reported to make it possible to isolate single individual neurons from neural tissues with well-preserved mRNA quality.[14,15] In addition, RNA amplification techniques preserving the relative amounts of individual mRNAs have been developed recently.[16,17] LCM and RNA amplification combined with DNA microarray analyses have been reported to enable studies of cell type–specific gene expression profiles in tissues with multiple cell lineages.[16,18] Such integrated analysis system provide an effective tool for investigating the cellular events affecting cell type–specific gene expression profiles in neurodegenerative diseases such as ALS. Indeed, we and other groups demonstrated that these integrated systems could be applied successfully to describe cell-specific gene expression profiles in neuronal tissues.[15,18]

In this study, we applied integrated LCM, RNA amplification, and DNA microarray analysis to clarify alterations of motor neuron–specific gene expression in sporadic ALS cases and successfully obtained expression gene database in situ from degenerating motor neurons in sporadic ALS spinal cord.

## Patients and Methods

### *Tissues from Amyotrophic Lateral Sclerosis and Control Patients*

Fresh specimens of lumbar spinal cord (L4 to L5 segment) from 14 sporadic ALS patients (nine men, five women) and 13 neurologically normal patients (nine men, four women) were obtained at autopsy (Table 1). Diagnosis of ALS was

*Table 1. Details of Patients Examined in This Study*

| Patients | Sex | Age (yr) | Duration of Illness (yr) | Postmortem Delay (hr) | Diseases | Spinal Cord Neuropathology Motor Neuron Loss/Gliosis |
|---|---|---|---|---|---|---|
| ALS1 | M | 72 | 3.7 | 6 | ALS (B, UL, LL) | Moderate/mild |
| ALS2 | M | 71 | 2.3 | 5 | ALS (LL, UL) | Moderate/mild |
| ALS3 | M | 58 | 1.8 | 13 | ALS (UL, LL, B) | Severe/severe |
| ALS4 | M | 43 | 2.6 | 5 | ALS (LL, B) | Moderate/mild |
| ALS5 | M | 53 | 2.8 | 11 | ALS (B, UL, LL) | Moderate/severe |
| ALS6 | F | 79 | 4.0 | 4 | ALS (UL, LL, B) | Severe/severe |
| ALS7 | F | 59 | 2.5 | 3 | ALS (UL) | Mild/mild |
| ALS8 | F | 67 | 2.0 | 7 | ALS (UL, B) | Severe/mild |
| ALS9 | M | 74 | 4.3 | 10 | ALS (LL, B) | Severe/mild |
| ALS10 | F | 47 | 1.8 | 4 | ALS (B, UL, LL) | Mild/mild |
| ALS11 | M | 74 | 4.5 | 12 | ALS (UL, LL) | Moderate/mild |
| ALS12 | M | 57 | 3.5 | 5 | ALS (LL, UL) | Severe/mild |
| ALS13 | F | 53 | 3.0 | 8 | ALS (B, UL, LL) | Severe/severe |
| ALS14 | M | 63 | 2.2 | 5 | ALS (UL, B) | Mild/mild |
| Control1 | M | 57 | — | 7 | Pneumonia | No |
| Control2 | M | 78 | — | 10 | Cerebral infarction | No |
| Control3 | M | 72 | — | 9 | Lung cancer | No |
| Control4 | F | 52 | — | 7 | Pneumonia | No |
| Control5 | F | 65 | — | 12 | Pneumonia | No |
| Control6 | M | 75 | — | 10 | Heart failure | No |
| Control7 | M | 42 | — | 5 | Heart failure | No |
| Control8 | F | 76 | — | 5 | Pancreas cancer | No |
| Control9 | F | 84 | — | 6 | Myocardial infarction | No |
| Control10 | M | 48 | — | 13 | Heart failure | No |
| Control11 | M | 77 | — | 11 | Heart failure | No |
| Control12 | M | 66 | — | 11 | Cerebral infarction | No |
| Control13 | M | 75 | — | 4 | Pneumonia | No |

The age, duration of illness, and postmortem delay are indicated for the ALS and control cases. Predominant clinical features of ALS are shown: UL = upper limbs; LL = lower limbs; B = bulbar. Neuropathological involvement of spinal cords was graded as previously. Ten ALS samples were used for microarray analysis: five of them (1, 7, 10, 11, and 14) were analyzed using 4.8K array for spinal motor neurons; five (2, 4, 5, 8, and 12) using 1.0K for spinal motor neurons; five (1, 3, 10, 13, and 14) using 4.8K for spinal ventral horn gray matter; and five (1, 2, 4, 5, and 13) and five (1, 2, 7, 8, and 10) control samples using 4.8K and 1.0K. Thirteen ALS (1–13) and 11 (1–11) control samples were used for TaqMan reverse transcription polymerase chain reaction analysis. Five ALS (1, 10, 11, 13, and 14) and four control (1, 3, 5, and 12) samples were used for in situ hybridization and immunohistochemistry.
ALS = amyotrophic lateral sclerosis.

confirmed by El Escorial diagnostic criteria defined by the World Federation of Neurology and the histopathological findings, particularly the presence of the Bunina body.[2,3] All cases of ALS were sporadic and did not show any heredity. ALS patients with *SOD1* mutation were excluded. The collection of tissues and their use for this study were approved by the ethics committee of Nagoya University Graduate School of Medicine. Tissues were frozen immediately and stored at −80°C until use. The mean ages and standard deviations for ALS and control patients were 62.1 ± 11.0 and 66.7 ± 13.1 years, and the mean postmortem intervals and standard deviations were 7.0 ± 3.3 and 8.5 ± 3.0 hours, respectively. The differences between the means of either age or postmortem interval were not significant between the ALS and control groups. The cause of death in all ALS patients was respiratory failure, and the causes in the control patients were pneumonia, lung cancer, or acute heart failure (see Table 1). Parts of the lumbar spinal cord were fixed in 10% buffered formalin solution, and processed for paraffin sections. The sections were stained with hematoxylin and eosin and Klüver-Barrera and Holzer techniques, and histological assessment was performed. The degree of motor neuron loss and astrogliosis was ranked as mild, moderate or severe according to previously reported.[19,20]

### *Laser-Captured Microdissection of Spinal Motor Neurons*

Sections (10μm) were cut with a standard cryostat, mounted on poly-L-lysin coated slides (Zeiss, Thornwood, NY), and stained with hematoxylin to identify the motor neurons located in the medial and lateral nuclei of the ventral horns of lumber spinal cords. After staining with hematoxylin, the sections were washed in RNase-free water and dried.[21,22] The PALM Robot-Microbeam system (P.A.L.M. Mikrolaser Technology AG, Bernried, Germany) was used for laser capture. The pulsed laser microbeam cut precisely around the targeted motor neurons in the spinal ventral horn (LCM; see Fig 1A–C). The identity of motor neurons was ascertained by reverse transcription polymerase chain reaction (RT-PCR) for choline acetyltransferase (ChAT) as described previously.[15] Each laser-isolated specimen subsequently was ejected from the glass slide with a single or several laser shots and collected directly into the cap of a PCR tube containing denaturing buffer by a process of laser pressure catapulting in the totally noncontact manner previously described.[23] The LCM-isolated cells (approximately 500 pooled cells) were dissolved in denaturing buffer (StrataPrep Total RNA Microprep Kit; Stratagene, San Diego, CA) and stored at −80°C until use.

### *RNA Extraction of Laser-Captured Microdissection Motor Neuron Samples and Spinal Ventral Horn Homogenates*

LCM-isolated cells in denaturing buffer were thawed and centrifuged briefly before the RNA was extracted using a StrataPrep Total RNA Microprep Kit (Stratagene) according to the manufacturer's protocol. RNA was extracted as well from the total homogenates of ventral horn gray matter of spinal cords,[19] which was dissected under a dissecting microscope.

### *Reverse Transcription and T7 RNA Polymerase Amplification of RNA*

Ten microliters of purified RNA obtained as described above was mixed with 1μl of 0.5μg/ml T7-oligodT primer (5′-TCTAGTCGACGGCCAGTGAATTGTAATACGACTCACTATAGGGCGT$_{21}$-3′) to initiate first-strand synthesis. The primer and RNA were incubated in 4μl of 5 × first-strand reaction buffer, 0.1M DTT (2μl), 10mM dNTPs (1μl), 1μl of RNasin, and 1μl of Superscript II reverse transcriptase (Invitrogen, Carlsbad, CA) at 42°C for 1 hour, and then 30μl of 5 × second-strand synthesis buffer, 10mM dNTPs (3μl), 4μl of DNA polymerase, 1μl of *Escherichia coli* RNase H, and 1μl of *E. coli* DNA ligase and 91μl of RNase-free $H_2O$ were added, and the mixture was incubated at 16°C for 2 hours and then at 16°C for 10 minutes after the addition of 2μl of T4 DNA polymerase. Next, an Ampliscribe T7 Transcription Kit (Epicentre Technologies, Madison, WI) was used for RNA amplification: 8μl double-stranded cDNA, 2μl of 10 × Ampliscribe T7 buffer, 1.5μl each of 100mM ATP, CTP, GTP, and UTP, 0.1 M DTT (2μl), and 2μl of T7 RNA polymerase were incubated at 42°C for 3 hours.

For second-round amplification, 10μl of amplified RNA (aRNA) from first-round amplification was mixed together with 1μl of 1mg/ml random hexamers (Invitrogen), and then first-stranded cDNA was synthesized, followed by second-stranded cDNA synthesis as described above. The double-stranded cDNA was subjected to second-round T7 in vitro transcription as above and then subsequent third-round aRNA amplification. After third-round amplification, aRNA was treated with DNase (Wako, Kanagawa, Japan) and cleaned up using an RNeasy Kit (Qiagen, Valencia, CA) according to the manufacturer's protocol.

### *DNA Microarray Analysis*

Fluorescent cDNA probes were synthesized from aRNA of laser-captured spinal motor neurons and RNA from ventral spinal tissue homogenates using an Atlas Glass Fluorescent Labeling Kit (Clontech, Palo Alto, CA) according to the manufacturer's protocol. Cy3-labeled cDNA probes were synthesized from ALS samples for spinal motor neurons and homogenates, and Cy5-labeled cDNA probes were synthesized from control samples. BD Atlas Glass Microarray Human 1.0 and 3.8 (Clontech) slides were hybridized with these fluorescent labeled probes overnight at 50°C and then washed four times and dried according to the manufacturer's protocol. Individual Cy3-labeled cDNA probes from ALS RNA samples of spinal motor neurons and homogenates for each patient were coupled with Cy5-labeled cDNA probes from control RNA samples of those tissues, which were prepared by mixing equal amounts of RNA samples amplified from the control patients. The microarrays were scanned in a laser scanner (GenePix 4000; Axon Instruments, Union City, CA), and the resulting signals were quantified and stored using GenePix Pro analysis software (Axon Instruments). The data for each expressed gene obtained from microarray analysis were expressed as the ratios of the values of individual ALS patients or the means of the values of ALS to the values of the control patients. The values of gene expression levels were means-calculated from motor neurons of 5 or 10 inde-

pendent individuals with ALS as well as from spinal ventral horns of 5 individuals with ALS.

*Quantitative Real-Time Reverse Transcription Polymerase Chain Reaction*

The probe and primers for the real-time PCR were designed using Primer3′ (S. Rozen and H. J. Skaletsky, available at http://www-genome.wi.mit.edu/genome_software/other/primer3.html). TaqMan PCR was conducted using an iCycler system (Bio-Rad Laboratories, Hercules, CA) with a QuantiTect Probe PCR Kit (Qiagen) and the cDNA according to the manufacturer's protocol. The reaction conditions were 95°C for 3 minutes and then 50 cycles of 15 seconds at 95°C followed by 60 seconds at 55°C. All experiments were performed in quadruplicate, and several negative controls were included. For an internal standard control, the expression of glyceraldehyde-3-phosphate dehydrogenase (GAPDH) was simultaneously quantified. The primers and probe sequences for the examined genes (acetyl-CoA transporter: D88152; Bak: NM_001188; CRABP1: NM_004378; cyclin C: M74091; dynactin 1: NM_004082; EGR3: NM_004430; ephrin A1: M57730; GAPDH: NM_002046; KIAA0231: D86984; and TrkC: U05012) were described in the legends for Figure 3. The threshold cycles of each gene were determined as the number of PCR cycles at which the increase in reporter fluorescence reached 10 times above the baseline signal. The weight ratio of the target gene to GAPDH gives the standardized expression level.

*In Situ Hybridization*

Frozen sections (10μm thick) of the spinal cord were prepared and immediately fixed in 4% paraformaldehyde. Then, they were treated with 0.1% diethylpyrocarbonate (DEPC) twice for 15 minutes and prehybridized at 45°C for 1 hour. Digoxigenin-labeled cRNA probes were generated from linearized plasmids for the genes of interest using SP6 or T7 polymerase (Roche Diagnostics, Basel, Switzerland). Gene names, Genebank accession number, probe position (nucleotide number), and probe size were as follows: acetyl-CoA transporter, D88152, nucleotides 397-741, 345bp; Bak, NM_001188, nucleotides 792–2094, 345bp; CRABP1, NM_004378, nucleotides 210–545, 336bp; dynactin 1, NM_004082, nucleotides 2392–2774, 383bp; DR5, NM_004082, nucleotides 682–1070, 389bp; EGR3, NM_004430, nucleotides 1433–1794, 362bp; KIAA0231, D86984, nucleotides 698–1053, 356bp; TrkC, U05012, nucleotides 1412–1721, 310bp. After prehybridization, the sections were hybridized with each digoxigenin-labeled cRNA probe overnight at 45°C. The washed sections were incubated with alkaline phosphatase-conjugated anti–digoxigenin antibody (Roche Diagnostics). The signal was visualized with NBT/BCIP (Roche Diagnostics).

*Immunohistochemistry*

Frozen sections (10μm thick) of the spinal cord were prepared and immediately fixed in 4% paraformaldehyde. Then, they were blocked with 2% bovine serum albumin (Sigma) in Tris-buffered saline at room temperature for 20 minutes and incubated with anti–cyclin C (1:200 dilution; Santa Cruz Biotechnology, Santa Cruz, CA) antibody overnight at 4°C. Subsequent procedures were performed using ENVISION++KIT/HRP (diaminobenzidine tetrahydrochloride; DAKO, Carpinteria, CA) according to the manufacturer's protocol.

*Statistical Analyses*

To assess the correlation of intensity values for each labeling sample, we used scatterplots and measured linear relationships. The correlation coefficient, $R^2$, that was calculated indicates the variability of intensity values between Cy-5– and Cy-3–labeled samples. To perform cluster analyses of hierarchical clustering, self-organizing maps (SOM) and principal component analysis after logarithmic transformation, we used Acuity 3.0 software (Axon Instruments). The data measured by quantitative real-time RT-PCR analysis were analyzed by Student's $t$ tests.

## Results

*T7 Amplification Preserves Gene Expression Profiles*

Because the amounts of laser-microdissected samples were extremely low and did not contain enough mRNA for further analysis, RNA amplification was required. It was critical to achieve sufficient RNA amplification and yet maintain the expression profiles of mRNAs. We performed experiments to determine how the expression profiles of mRNAs were affected by the T7 amplification procedure. RNA samples were extracted from control spinal cords and a part of RNA samples was amplified using T7 amplification. One flourescently labeled probe was synthesized from an individually amplified RNA (aRNA) or nonamplified RNA (nRNA) and was hybridized to microarrays. Independent amplification of RNA yielded quite similar expression patterns. The correlation of signal intensities between independent amplifications for the third aRNA was $R^2 = 0.9157$, $p < 0.0001$, and on the other hand, the correlation of signal intensities in nRNA was $R^2 = 0.9157$, $p < 0.0001$ (Fig 1D, E). Previous reports using similar amplification procedures as ours also have confirmed the reproducibility of T7 amplification for the preservation of RNA expression profiles.[14,15,17] In this study, the third-round amplification was performed for the LCM-isolated motor neurons, but for the spinal ventral horn homogenates a single amplification produced enough RNA for further analysis, and similar expression patterns were found between the first and third amplifications (data not shown).

*Gene Expression Database of Spinal Motor Neurons and Ventral Horn Homogenates of Amyotrophic Lateral Sclerosis*

aRNA samples from the motor neurons and the ventral horn homogenates from the lumbar spinal cords were subjected to microarray analysis. The differences of the gene expression levels between ALS and control sam-

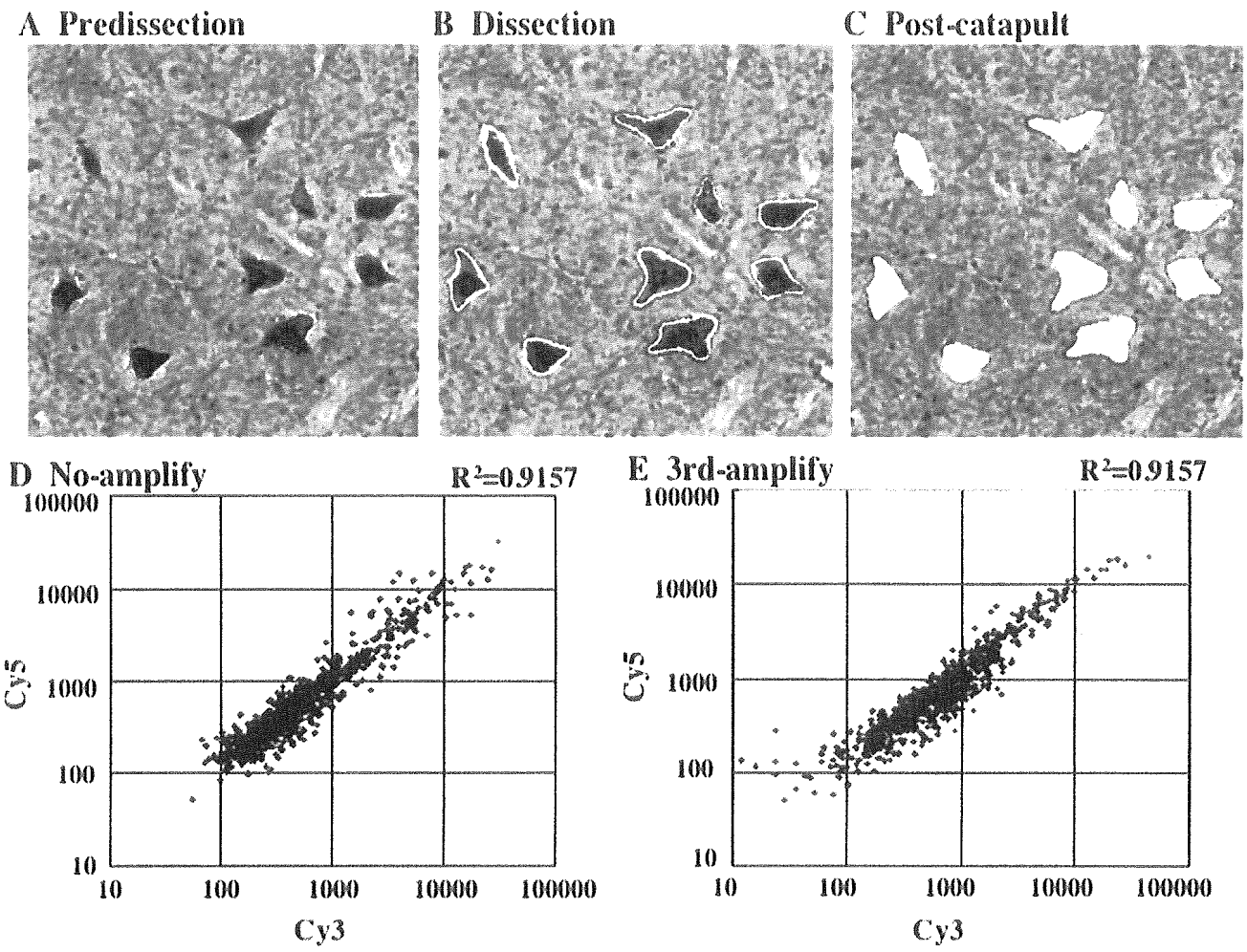


*Fig 1. Verification of laser-captured microdissection (LCM) and RNA amplification. Microdissection of motor neurons in spinal ventral horn: sections were stained with hematoxylin (A); margins of motor neurons were dissected by the laser beam (B); and motor neurons were isolated from slides by laser pressure catapulting (C). Scatterplots of nonamplified and amplified RNAs: correlations between independent amplifications of control spinal cord samples are shown using nonamplified (D) and third amplified RNAs (E). These RNAs were split into two samples for labeling of Cy5 and Cy3 and hybridized separately to two microarrays. The very high squared correlations reflect the high reproducibility of the hybridization results with the same values between nonamplified and third amplified RNAs.*

ples were expressed as ratios of the values of ALS individuals compared with the mean values of the controls. One percent (52/4,845) of genes examined were significantly upregulated in spinal motor neurons of ALS patients and 3% (144/4,845) were downregulated, assuming that the changes of 3.0-fold increase and 0.3-fold decrease were significant, when the mean levels of gene expression were calculated. In contrast with motor neurons, the total spinal ventral horn homogenates demonstrated 0.7% (37/4,845) and 0.2% (8/4,845) significant upregulation and downregulation of gene expression, respectively.

The genes prominently altered in ALS are listed in Tables 2 to 5 for spinal motor neurons and spinal ventral horn homogenates, respectively. Several upregulated genes listed were overlapping between spinal motor neurons (see Table 2) and ventral horns (see Table 4), suggesting that motor neuron overexpression is reflected to some extent by gene expression in ventral horn homogenates. The other genes upregulated in motor neurons were not present in the list for spinal ventral horns, because these gene expression changes were diluted and masked by changes occurring in other cell types. Because the number of spinal motor neurons was decreased in ALS spinal cords, most genes that were listed as downregulated genes in motor neurons (see Table 3) were not found in spinal ventral horns (see Table 5) except for three genes (CRABP1, EGR3, and postmeiotic segregation increased 2-like 11). When we categorized these altered genes in ALS motor neurons into several functional groups, the genes related to cell receptors and intracellular signaling, transcription,

*Table 2. Upregulated Genes in ALS Motor Neurons (Top 30)*

| GeneBank No. | Gene Name | Fold Change (ALS/control) |
|---|---|---|
| NM_003419 | Zinc finger protein 10 (KOX 1) | 8.86 |
| U91618 | Neurotensin/neuromedin N precursor | 8.33* |
| NM_004651 | Ubiquitin-specific protease 11 | 8.13 |
| D86984 | KIAA0231 | 7.31* |
| A26792 | Ciliary neuronotrophic factor (CNTF) | 6.76 |
| M77830 | Desmoplakin I & II (DSP; DPI & DPII) | 6.10 |
| NM_005622 | SA (rat hypertension-associated) homolog | 5.47 |
| NM_004733 | Acetyl-coenzyme A transporter | 5.33 |
| NM_000021 | Presenilin 1 (Alzheimer disease 3) | 4.96 |
| K03020 | Phenylalanine-4-hydroxylase (PAH) | 4.95* |
| AF016268 | Death receptor 5 (DR5); cytotoxic TRAIL receptor, TNFR10b | 4.91* |
| M74091 | G1/S-specific cyclin C (CCNC) | 4.82* |
| NM_000275 | Oculocutaneous albinism II | 4.78 |
| AF000936 | SH3-binding protein 2 | 4.73* |
| NM_000384 | Apolipoprotein B | 4.70 |
| M63099 | Interleukin-1 receptor antagonist | 4.66* |
| M57730 | Ephrin-A1 | 4.57* |
| L19067 | NF-κ B transcription factor p65 subunit | 4.52* |
| U66838 | Cyclin A1 (CCNA1) | 4.51* |
| NM_005021 | Ectonucleotide pyrophosphatase/phosphodiesterase 3 | 4.48 |
| NM_001550 | Interferon-related developmental regulator 1 | 4.45 |
| L25851 | Integrin alpha E precursor (ITGAE) | 4.43* |
| X16416 | C-abl1 protooncogene | 4.41 |
| U08015 | Transcription factor NF-ATc | 4.40* |
| U44378 | Mothers against dpp homolog 4 (SMAD4) | 4.35* |
| NM_005067 | Seven in absentia (Drosophila) homolog 2 | 4.22 |
| J04536 | Leukosialin precursor; sialophorin | 4.19* |
| X06745 | DNA polymerase alpha catalytic subunit | 4.15* |
| U09564 | Serine kinase | 4.09* |
| U37139 | β 3-endonexin | 4.06* |

Gene expression levels are expressed as means of fold-change, which is calculated by dividing the signals of each ALS sample by those of control samples, in the 5 or 10 (denoted by asterisk) patients with ALS.
ALS = amyotrophic lateral sclerosis.

metabolism, and cytoskeletal architecture were downregulated. The functional categories of secreted and extracellular communication proteins and cell cycle regulators were characteristically upregulated. A complete list of the differentially expressed genes is available online at http://www.med.nagoya-u.ac.jp/neurology/index.html.

*Differential Gene Expression Profiles between Spinal Motor Neurons and Ventral Horn Homogenates of Amyotrophic Lateral Sclerosis*

To compare the expression profile of motor neurons with that of spinal ventral horn homogenates, we performed cluster analyses. Because the patterns of gene expression from microarray analysis are impossible to discern by eye, data analysis software (Acuity 3.0 software; Axon Instruments) was used based on the dimensionality of the data: hierarchical clustering for high dimensional gene space and principal component analysis and SOM for low one. Hierarchical clustering clearly discriminated the expression profile of isolated motor neurons from that of ventral horn homogenates, showing two grouped branches of the dendrogram with a correlation coefficient of 0.446 (Fig 2A). Moreover, a principal component analysis confirmed the distinction of gene expression profiles between spinal motor neurons and ventral horns (see Fig 2B). The gene expression profile of motor neurons was clustered into a single cluster by the two clustering algorithms, which was well separated from that of spinal ventral horn gray matter, suggesting a relatively uniform degenerating process in spinal motor neurons in ALS.

*Motor Neuron–Specific Gene Expression Profiles Identified by the Self-Organizing Map Analysis*

To further analyze the expression pattern specific to spinal motor neurons, a SOM was produced as a nonhierarchical clustering.[24,25] The examined genes were subdivided into 25 clustered categories, and the selected genes are shown in a certain group of the SOM (see Fig 2C, Table 6). The genes contained in the clusters reflect the expression pattern in spinal motor neurons as well as that in spinal ventral horns, and these selected genes are somehow different from those in Tables 2 to 5 because of the different bases of classification. Clustering of the SOM showed motor neu-

*Table 3. Downregulated Genes in ALS Motor Neurons (Bottom 30)*

| GeneBank No. | Gene Name | Fold Change (ALS/control) |
|---|---|---|
| NM_004378 | Cellular retinoic acid–binding protein 1 (CRABP1) | 0.12 |
| NM_004430 | Early growth response 3 (EGR3) | 0.14 |
| NM_005558 | Ladinin 1 | 0.15 |
| NM_003603 | Arg/Abl-interacting protein ArgBP2 | 0.15 |
| NM_000117 | Emerin (Emery-Dreifuss muscular dystrophy) | 0.15 |
| NM_004357 | CD151 antigen | 0.15 |
| X06820 | Ras homolog gene family member B (RHOB) | 0.15* |
| NM_003834 | Regulator of G-protein signalling 11 | 0.16 |
| NM_002960 | S100 calcium-binding protein A3 | 0.16 |
| NM_006289 | Talin | 0.16 |
| NM_000964 | Retinoic acid receptor, α | 0.17 |
| NM_002391 | Midkine | 0.17 |
| M96944 | Paired box protein PAX-5 | 0.17* |
| M74178 | Hepatocyte growth factor–like protein | 0.17* |
| NM_003822 | Nuclear receptor subfamily 5, group A, member 2 | 0.17 |
| NM_001188 | BCL2-antagonist/killer 1; Bak | 0.18 |
| NM_000733 | CD3E antigen, epsilon polypeptide (TiT3 complex) | 0.18 |
| NM_000408 | Glycerol-3-phosphate dehydrogenase 2 (mitochondrial) | 0.18 |
| NM_000156 | Guanidinoacetate *N*-methyltransferase | 0.18* |
| M11886 | Major histocompatibility complex, class I, C | 0.18* |
| NM_003865 | Homeo box (expressed in ES cells) 1 | 0.18 |
| M36340 | ADP-ribosylation factor 1 (ARF1) | 0.18* |
| NM_001725 | Bactericidal/permeability-increasing protein | 0.18 |
| NM_005334 | Host cell factor C1 (VP16-accessory protein) | 0.19 |
| NM_004192 | Acetylserotonin *O*-methyltransferase–like | 0.19 |
| NM_002684 | Postmeiotic segregation increased 2–like 11 | 0.19 |
| M11233 | cathepsin D precursor (CTSD) | 0.19* |
| NM_002313 | Actin binding LIM protein 1 | 0.19 |
| NM_002196 | Insulinoma-associated 1 | 0.19 |
| NM_002277 | Keratin, hair, acidic, 1 | 0.19 |

Gene expression levels are expressed as means of fold-change, which is calculated by dividing the signals of each ALS sample by those of control samples, in the 5 or 10 (denoted by asterisk) patients with ALS.
ALS = amyotrophic lateral sclerosis.

ron–specific upregulated and downregulated gene expression commonly observed in five patients.

Clusters 1 (SOM1) and 6 (SOM6) contains 110 and 169 genes, respectively, that generally are downregulated in spinal motor neurons in all five cases examined, and those are known to be involved in the functional category of cell surface antigens and cell receptors, transcription, and cytoskeleton, whereas clusters 24 (SOM24) and 25 (SOM25) have 191 and 93 genes, respectively, that are predominantly upregulated in spinal motor neurons in all cases and belong to the functional category of cell signaling with extracellular communication, and cell death–associated proteins. The pattern of subcellular localization of their gene products also confirms the characteristics of the functional categories of upregulated and downregulated genes, that is, that plasma membrane and cytoskeletal proteins are more downregulated, and extracellular secreted proteins are more upregulated, in ALS motor neurons. All the genes listed in Table 3 are included in SOM1 and SOM6, whereas SOM24 and SOM25 do not contain all of the genes listed in Table 2. The former group of genes, with downregulation in motor neurons, included BCL2-antagonist/killer 1 (Bak) and TrkC receptor. Regarding genes related to transcription, early growth response 3 (EGR3), cellular retinoic acid–binding protein 1 (CRABP1), retinoic acid receptors, and Musashi 1 were included in SOM1 and SOM6 as downregulated genes. The expression of dynactin and microtubule-associated proteins (MAPs), which belong to the functional category of cytoskeleton and axonal transport, was downregulated in ALS motor neurons. On the other hand, KIAA0231 and acetyl-coenzyme A transporter were classified into the upregulated genes in motor neurons of ALS. Regarding genes related to cell death, the expression of cyclins A1 and C, death receptor 5 (DR5), and interleukin-1 receptor antagonist was upregulated together with that of NF-κB, tumor necrosis factor (TNF) receptor–associated factor 6 (TRAF6), and caspase-1, -3, and -9 in SOM24 and SOM25. For genes in the category of trophic factor cell signaling with extracellular communication, CNTF, HGF, and glial cell line–derived neurotrophic factor (GDNF) were upregulated in ALS motor neurons, whereas midkine was downregulated. The expression of vascular endothelial growth factor as

*Table 4. Upregulated Genes in Spinal Ventral Horns of ALS (Top 30)*

| GeneBank | Gene Name | Fold Change (ALS/control) |
|---|---|---|
| NM_000508 | Fibrinogen, A α polypeptide | 8.23 |
| D86984 | KIAA0231 | 6.09 |
| NM_001801 | Cysteine dioxygenase, type I | 5.81 |
| X02544 | α-1-Acid glycoprotein 1 precursor | 5.59 |
| NM_001973 | ELK4, ETS-domain protein (SRF accessory protein 1) | 5.12 |
| NM_000021 | Presenilin 1 (Alzheimer disease 3) | 5.00 |
| NM_002097 | General transcription factor IIIA | 4.96 |
| U08015 | Transcription factor NF-ATc | 4.96 |
| M57730 | Ephrin-A1 | 4.88 |
| U91618 | Neurotensin/neuromedin N precursor | 4.79 |
| AF000936 | SH3-binding protein 2 | 4.50 |
| NM_002949 | Mitochondrial ribosomal protein L12 | 4.11 |
| NM_002386 | Melanocortin 1 receptor | 4.03 |
| NM_001991 | Enhancer of zeste (Drosophila) homolog 1 | 3.93 |
| NM_000947 | Primase, polypeptide 2A (58kDa) | 3.92 |
| NM_000239 | Lysozyme (renal amyloidosis) | 3.88 |
| NM_001550 | Interferon-related developmental regulator 1 | 3.67 |
| NM_004602 | Staufen (Drosophila, RNA-binding protein) | 3.66 |
| NM_000063 | Complement component 2 | 3.58 |
| NM_004651 | Ubiquitin-specific protease 11 | 3.54 |
| NM_000397 | Cytochrome b-245, β polypeptide | 3.51 |
| NM_002056 | Glutamine-fructose-6-phosphate transaminase 1 | 3.41 |
| L25851 | Integrin α E precursor (ITGAE) | 3.36 |
| NM_004616 | Transmembrane 4 superfamily member 3 | 3.21 |
| NM_003720 | Down syndrome critical region gene 2 | 3.18 |
| J04536 | leukosialin precursor; sialophorin | 3.15 |
| X06745 | DNA polymerase alpha catalytic subunit | 3.15 |
| K03020 | Phenylalanine-4-hydroxylase (PAH) | 3.14 |
| NM_001329 | C-terminal binding protein 2 | 3.14 |
| NM_000276 | Oculocerebrorenal syndrome of Lowe | 3.13 |

Gene expression levels are expressed as means of fold-change, which is calculated by dividing the signals of each ALS sample by those of control samples, in the five patients with ALS.
ALS = amyotrophic lateral sclerosis.

well as NT-3 was unchanged. Furthermore, the genes whose expression was altered significantly in spinal ventral horn homogenates as shown in Tables 4 and 5 showed similar alterations to some extent in the remaining motor neurons. However, the upregulated genes, such as integrin αE and sialophorin for cell adhesion, which were demonstrated to be spinal ventral horn–derived (see Table 4) as well as spinal motor neuron–derived (Table 2) genes, were not sorted out into SOM24 and SOM25, indicating that their upregulation occurred predominantly in glial cells.

### *Data Confirmation with Quantitative Real-Time Reverse Transcription Polymerase Chain Reaction, In Situ Hybridization, and Immunohistochemistry*

To assure the validity of the gene expression levels detected by microarray analysis, we performed quantitative real-time RT-PCR analysis on some genes of interest using a TaqMan PCR system. Because LCM-isolated motor neurons did not contain enough RNA to perform real-time RT-PCR analysis, only selected genes were assessed in motor neurons, and for other genes the spinal ventral horn homogenates were used as the template for quantitative RT-PCR. When the extent of increase or decrease of gene expression levels was expressed as the ratio of the genes of interest to GAPDH, acetyl-CoA transporter and KIAA0231 were significantly increased 3.1-fold ($p < 0.001$) and 3.3-fold ($p < 0.01$) in spinal motor neurons of ALS, respectively (Fig 3). EGR3 expression decreased to 0.27-fold ($p < 0.01$) in ALS motor neurons. These mRNA alterations were also detected at comparable levels when using spinal ventral horn homogenates of ALS (acetyl-CoA transporter, 1.8-fold increase [$p < 0.005$]; KIAA0231, 2.3-fold increase [$p < 0.05$]; and EGR3, 0.41-fold decrease [$p < 0.01$]). In addition, the gene expression of Bak and TrkC was downregulated 0.53-fold ($p < 0.01$) and 0.40-fold ($p < 0.05$) in ALS, respectively. Moreover, increases of ephrin A1 and cyclin C expression were observed to the extents of 2.5-fold ($p < 0.05$) and 4.9-fold ($p < 0.01$), whereas dynactin 1 mRNA was downregulated 0.44-fold ($p < 0.01$), and CRABP1 mRNA was also downregulated to 0.59-fold ($p < 0.01$) in ALS.

To further verify the localization and extent of expression of genes of interest, we performed in situ hy-

*Table 5. Downregulated Genes in Spinal Ventral Horns of ALS (Bottom 30)*

| GeneBank | Gene Name | Fold Change (ALS/control) |
|---|---|---|
| NM_000843 | Glutamate receptor, metabotropic 6 | 0.22 |
| NM_000730 | cholecystokinin A receptor | 0.24 |
| NM_003134 | Signal recognition particle 14kDa | 0.26 |
| NM_003163 | Syntaxin 1B | 0.27 |
| NM_006476 | ATP synthase, H+ transporting, mitochondrial F1F0, subunit g | 0.27 |
| NM_001610 | Acid phosphatase 2, lysosomal | 0.28 |
| NM_003108 | SRY (sex determining region Y)-box 11 | 0.29 |
| NM_001446 | Fatty acid binding protein 7, brain | 0.30 |
| NM_004583 | RAB5C, member RAS oncogene family | 0.31 |
| NM_001125 | ADP-ribosylarginine hydrolase | 0.31 |
| NM_003320 | Tubby (mouse) homolog | 0.31 |
| NM_001731 | B-cell translocation gene 1, antiproliferative | 0.31 |
| NM_000999 | Ribosomal protein L38 | 0.32 |
| NM_004128 | General transcription factor IIF, polypeptide 2 (30kDa subunit) | 0.32 |
| NM_001765 | CD1C antigen, c polypeptide | 0.32 |
| NM_004430 | Early growth response 3 (EGR3) | 0.33 |
| K00558 | Tubulin, α, ubiquitous | 0.33 |
| NM_006732 | FBJ murine osteosarcoma viral oncogene homolog B | 0.33 |
| NM_002040 | GA-binding protein transcription factor, α subunit (60kDa) | 0.34 |
| NM_006161 | Neurogenin 1 | 0.35 |
| NM_002684 | Postmeiotic segregation increased 2–like 11 | 0.35 |
| NM_000801 | FK506-binding protein 1A (12kDa) | 0.35 |
| NM_001051 | Somatostatin receptor 3 | 0.35 |
| NM_005017 | Phosphate cytidylyltransferase 1, choline, alpha isoform | 0.36 |
| NM_004927 | Chromosome 11 open reading frame 4 | 0.36 |
| NM_000046 | Arylsulfatase B | 0.37 |
| NM_004378 | Cellular retinoic acid–binding protein 1 (CRABP1) | 0.37 |
| NM_001998 | Fibulin 2 | 0.38 |
| NM_001839 | Calponin 3, acidic | 0.38 |
| NM_001183 | ATPase, H+ transporting, lysosomal, subunit 1 | 0.39 |

Gene expression levels are expressed as means of fold-change, which is calculated by dividing the signals of each ALS sample by those of control samples, in the five patients with ALS.
ALS = amyotrophic lateral sclerosis.

bridization on selected genes. The mRNAs for acetyl-CoA transporter, KIAA0231, and EGR3 were localized in the remaining motor neurons (Fig 4). Spinal motor neurons overexpressed acetyl-CoA transporter and KIAA0231 in ALS, whereas EGR3 was underexpressed. Moreover, TrkC, CRABP1, Bak, and dynactin 1 gene expression was found in motor neurons, and those signals were reduced in ALS. DR5 signals were increased in motor neurons in ALS. Cyclin C signals with punctate immunoreactivity were increased in the cytoplasm as well as in nuclei in ALS motor neurons. The nuclear staining of motor neurons for cyclin C was more prominent in ALS compared with controls.

## Discussion

Although reports about differential gene expression using the postmortem spinal cords, including those of patients with ALS, have been published,[26,27] the precise gene expression profiles of the degenerating motor neurons themselves have remained to be elucidated. Laser-captured dissection of motor neurons and subsequent microarray analysis are the most appropriate approaches to understanding the motor neuron–specific gene expression profile related to the motor neuron degeneration process in sporadic ALS, because these approaches eliminate bias of motor neuron loss, reactive astroglial proliferation, and other cellular reactions. Indeed, serine kinase has been reported to be underexpressed in ALS spinal cord gray matter,[27] but this study showed it was overexpressed in isolated motor neurons, suggesting that the reported underexpression in whole gray matter was influenced by the decreased motor neuron population. In contrast, cathepsin D expression was downregulated in the ALS motor neurons in this study, whereas it was increased in spinal cord gray matter in a previous report,[27] indicating its upregulation in glial cells. In addition, clustering analyses showed that the gene expression profile in the spinal motor neurons was substantially different from that in the whole homogenates of spinal ventral horn gray matter.

The overall microarray analysis using spinal ventral horn homogenates showed gene expression changes in less than 1% of genes examined with more genes showing increased than decreased expression. On the other hand, the motor neuron–specific microarray analysis

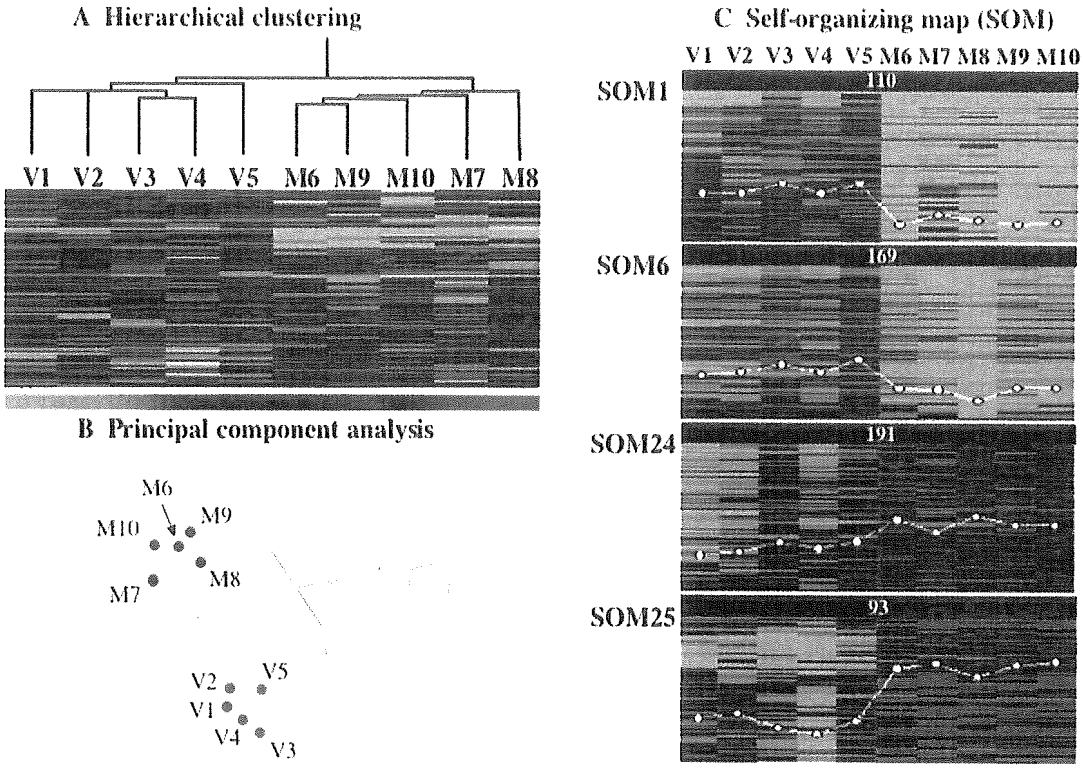


*Fig 2. Clustering of gene expression in spinal motor neurons and spinal ventral horns. (A) Hierarchical clustering of gene expression in spinal motor neurons and ventral horns. The dendrogram was produced by hierarchical clustering of relative expression levels of 4,845 genes (rows) in five spinal homogenate and five motor neuron samples (columns) in making a total of 48,450 data points. Visual representation is shown with green representing downregulated (<0.44), black representing intermediate, and red representing upregulated (>2.28). The hierarchical clustering successfully detects two large clusters of amyotrophic lateral sclerosis (ALS), discriminating between spinal homogenates of ventral horns (samples V1 [ALS1], V2 [ALS10], V3 [ALS3], V4 [ALS14], and V5 [ALS13]) and motor neurons (samples M6 [ALS1], M7 [ALS10], M8 [ALS14], M9 [ALS11], and M10 [ALS7]), with a correlation coefficient of 0.446 at the branching point. (B) Principal component analysis of spinal motor neurons and ventral horns. Principal component analysis by six components for the 4,845 genes shows two main clusters consisting of spinal motor neurons (M6–10) and homogenates (V1–5). The number of patients corresponds to those in the dendrogram. (C) Self-organizing map (SOM) analysis of spinal motor neurons and ventral horns. The 4,845 genes are grouped into 25 clusters, the optimal size of which is calculated from gap statistics analysis. In SOM1 and SOM6, most genes are downregulated and in SOM24 and SOM25 the majority of genes are upregulated commonly in isolated motor neurons of five cases (M6–10). The numbers of genes are given at the top, and selected genes are listed for clusters 1, 6, 24, and 25 in Table 6.*

showed that the proportion of significantly downregulated genes was 3% of the examined genes, whereas that of upregulated genes was one third of the downregulated genes. Moreover, the genes found to be downregulated specifically in motor neurons were not found to be downregulated in ventral horns, except for three genes with high expression levels. These results strongly support the notion that microarray analysis of laser-captured isolated spinal motor neurons has an advantage especially for the detection of motor neuron–specific downregulated transcripts.

In the differentially expressed genes, cell death–associated genes and genes related to cell signaling were characteristically upregulated in ALS motor neurons, whereas the genes categorized into cytoskeleton and transcription were downregulated. In the prominently altered genes of interest related to the cell death pathway, acetyl-coenzyme A transporter, which has been cloned and shown to encode a protein with multitransmembranous spanning domains,[28] was overexpressed in ALS motor neurons. Acetyl-CoA transporter functions as a cofactor for acetylation of gangliosides as well as vesicular transport of acetylcholine, which is synthesized from acetyl-CoA and choline. Acetylation has been documented to suppress proapoptotic activity of GD3 ganglioside, which increased in ALS neural tissues, as previously shown.[29,30] These results suggest that enhanced expression of acetyl-CoA transporter may be related to the antiapoptotic mechanism for cholinergic motor neuron degeneration in ALS.

*Table 6. Selected Genes Characterized by SOM (select each 15)*

| GeneBank | Gene Name | Fold Change (ALS/control) |
|---|---|---|
| SOM1/6: genes downregulated in ALS motor neurons | | |
| NM_002695 | Polymerase (RNA) II (DNA directed) polypeptide E (25kD) | 0.20 |
| M24857 | Retinoic acid receptor gamma 1 (RAR-γ 1) | 0.20 |
| NM_002375 | Microtubule-associated protein 4 | 0.20 |
| NM_001651 | Aquaporin 5 | 0.21 |
| NM_003178 | Synapsin II | 0.22 |
| NM_004624 | Vasoactive intestinal peptide receptor 1 | 0.23 |
| NM_001740 | Calbindin 2, (29kD, calretinin) | 0.24 |
| M73812 | G1/S-specific cyclin E (CCNE) | 0.25 |
| NM_003206 | Transcription factor 21 | 0.25 |
| NM_004082 | Dynactin 1 (p150) | 0.30 |
| U05012 | TRK-C; NT-3 growth factor receptor precursor | 0.31 |
| NM_003632 | Contactin associated protein 1 | 0.32 |
| NM_005910 | Microtubule-associated protein tau | 0.49 |
| NM_002373 | Microtubule-associated protein 1A | 0.51 |
| NM_002442 | Musashi (Drosophila) homolog 1 | 0.52 |
| SOM24/25: genes upregulated in ALS motor neurons | | |
| M60718 | Hepatocyte growth factor (HGF) | 3.42 |
| L20814 | Glutamate receptor subunit 2 (GLUR-2) | 3.34 |
| K02268 | β-neoendorphin-dynorphin precursor | 3.13 |
| L19063 | Glial cell line–derived neurotropic factor (GDNF) | 3.08 |
| NM_005543 | Insulin-like 3 | 2.79 |
| J04088 | DNA topoisomerase II alpha (TOP2A) | 2.58 |
| M22489 | Bone morphogenetic protein 2A (BMP2A) | 2.57 |
| U51004 | Hint protein; protein kinase C inhibitor | 2.26 |
| M87507 | Caspase 1, interleukin-1 β convertase precursor | 2.21 |
| NM_006196 | Poly(rC)-binding protein 1 | 2.16 |
| L29511 | Growth factor receptor–bound protein 2 | 2.04 |
| U78798 | TRAF6 | 1.98 |
| NM_001229 | Caspase 9, apoptosis-related cysteine protease | 1.89 |
| U84388 | Caspase and rip adaptor with death domain (CRADD) | 1.83 |
| U13737 | Caspase-3 | 1.77 |

Gene expression levels are expressed as means of fold-change, which is calculated by dividing the signals of each ALS sample by those of control samples, in the five patients with ALS. Genes listed in Tables 2 and 3 are excluded.
SOM = self-organizing map.

KIAA0231 was one of the mostly overexpressed genes in ALS motor neurons, but the function of this gene product is not known.

In the greatly downregulated genes of interest related to transcription, EGR3, whose expression was remarkably reduced in motor neurons of ALS, is a zinc-finger immediate-early transcription factor that is important for neurotrophin-3 (NT-3) regulation. It is known that EGR3 knockout mice develop gait ataxia, scoliosis, resting tremors, and ptosis due to the degeneration of muscle spindles, through disruption of NT-3 regulation.[31] In ALS motor neurons, TrkC receptor for NT-3 was underexpressed, whereas NT-3 expression was not changed. The finding about TrkC-null mutant and NT-3–null mutant mice show that NT-3-TrkC signaling is required to maintain Ia afferent central synapses of DRG neurons.[32] The marked downregulation of EGR3 in spinal motor neurons may disrupt sensory-motor connections by decreasing NT-3-TrkC signaling, resulting in motor neuron degeneration.

For neurotrophic support for ALS motor neurons, this study showed the overexpression of CNTF, GDNF, and HGF involved in the functional category of cell signaling, suggesting that these neurotrophic factors would be secondarily and compensatorily upregulated after motor neuron degeneration. Indeed, GDNF expression has been reported to increase in the spinal cords and decrease in the muscles of sporadic ALS patients.[33] In contrast with these neurotrophic factors, midkine was one of the significantly downregulated neurotrophic factors. Because midkine plays important roles in promotion of neuronal survival as well as modulation of neuromuscular junctions,[34] its underexpression may be related to motor neuron degeneration. In addition, the gene expression of vascular endothelial growth factor, which has been identified as a critical factor for motor neuron degeneration,[35–37] did not change significantly in gene expression in this study. SOD1 gene expression was not altered in spinal motor neurons and ventral horns. Moreover, the gene expres-

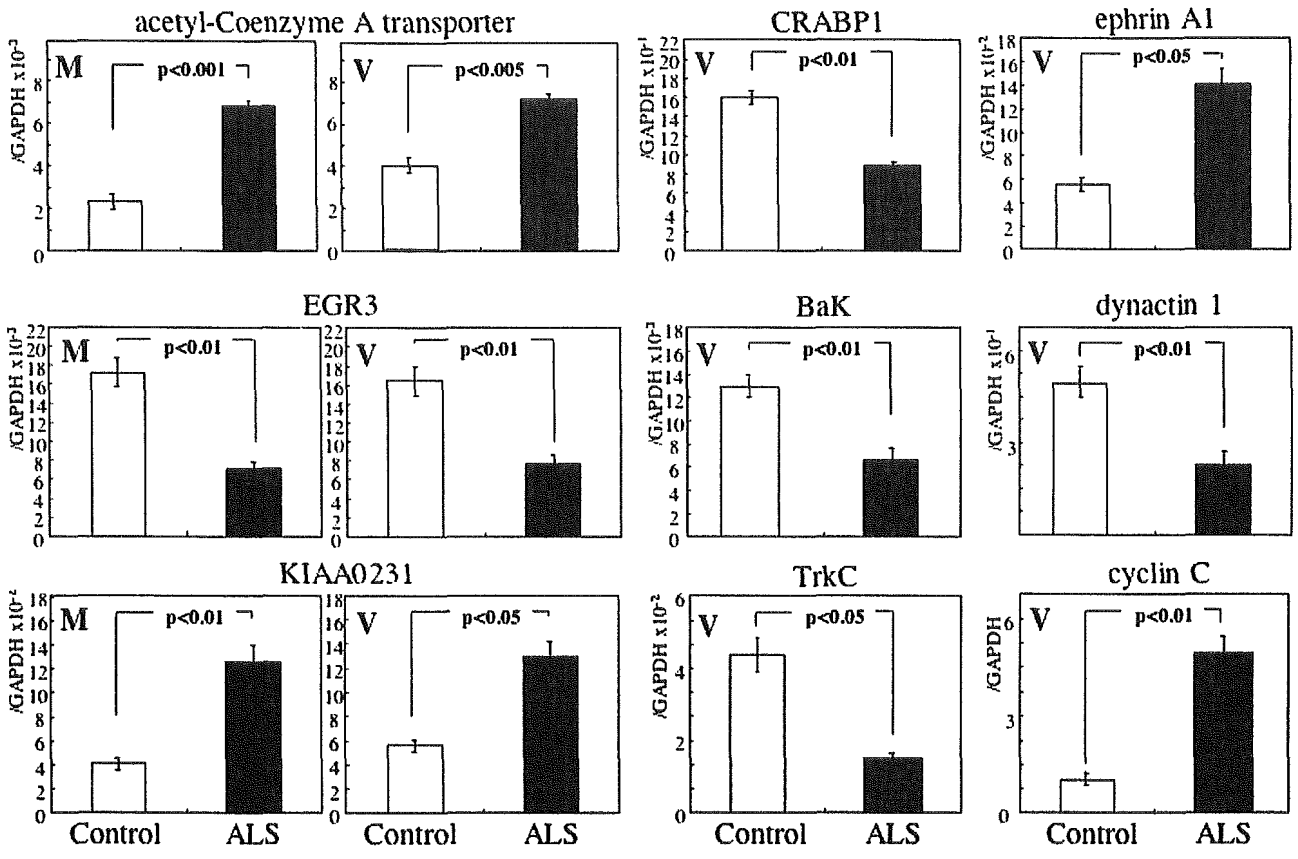


*Fig 3. Quantitative real-time reverse transcription polymerase chain reaction verification of the selected genes. Expression levels of acetyl-coenzyme A transporter, EGR3, KIAA0231, CRABP1, Bak, TrkC, ephrin A1, cyclin C, dynactin 1, and GAPDH were measured using spinal motor neurons (M) and ventral horns (V), and those of the target genes were normalized against the GAPDH level. The relative expression levels are expressed as mean ± standard error for 13 amyotrophic lateral sclerosis (ALS) cases and 11 controls. Gene names (Genebank accession number), primers and probe sequences (forward primer, reverse primer, and TaqMan probe; 5' to 3' sequence) were as follows: [acetyl-CoA transporter: D88152] (GGGTTACTTTTTGGGCAATG, AACGATTCCTCTGGGTTGAG, FAM-TTGGCCCTTGAATCTGCCGA-TAMRA); [Bak: NM_001188] (CTGGAAGATCAGCACCCTAAG, CCCCTCTCCTAGTAGGTCCTG, FAM-TGCTCCCATTCCTCCCTCCG-TAMRA); [CRABP1: NM_004378] (TGCAGGAGTTTAGCCACTTG, CTCACGGGTCCAGTAGGTTT, FAM- TGAGAACAAGATCCACTGCACCCA-TAMRA); [cyclin C: M74091] (TGAGCAGTGGAAGAATTTCG, ACCCTGCTCTCCTTCACTGT, FAM- TGCCAAAACCAAAACCACCTCCA-TAMRA); [dynactin 1: NM_004082] (ATGTGAATCGGGAACTGACA, GGGCCTTAGTCTCAGCAAAC, FAM- TGGAGAGGCAACAGCAGCCAC-TAMRA); [EGR3: NM_004430] (CTTCCCCATGATTCCTGACT, TTGAATGCCTTGATGGTCTC, FAM-TTCCAGGGCATGGACCCCAT-TAMRA); [ephrin A1: M57730] (GGCAAGGAGTTCAAAGAAGG, TCACCTTCAACCTCAAGCAG, FAM- CCATCCACCAGCATGAAGACCG-TAMRA); [GAPDH: NM_002046] (TCAAGAAGGTGGTGAAGCAG, GGTGTCGCTGTTGAAGTCAG, FAM-CCTCAAGGGCATCCTGGGCT-TAMRA); [KIAA0231: D86984] (CAACGGTCTTCCAGACAATG, GAGGTTGACCAGCTGTGAGA, FAM-TCCCAGAGGTGAAGCTGCCCTCTAMRA); and [TrkC: U05012] (TGAGAACCCCCAGTACTTCC, TCAGCACGATGTCTCTCCTC, FAM-CTGCCACAAGCCGGACACGT-TAMRA).*

sion level of GluR2 was upregulated, as shown by its classification in SOM25, but the expression of its editing enzyme (adenosine deaminase, RNA-specific, 2; ADAR2) was not altered in this study, although the editing efficiency of GluR2 mRNA has been demonstrated to be low in spinal motor neurons of ALS.[38]

Genes subject to transcriptional regulation constitute a crucial part of the whole human genome as demonstrated by human genome projects.[39] In addition to the gene expression of EGR3, the gene expression of retinoic acid receptor α and γ together with cellular retinoic acid–binding protein 1 (CRABP1), and Musashi 1, all of which are known to be inducers of neuronal differentiation,[40,41] was downregulated in spinal motor neurons of ALS. The dysregulation of retinoid receptor and retinol binding protein has been reported in the postmortem spinal cords of ALS and SOD1 mutant mice.[17,26] These interesting results imply the potential involvement of the differentiation signals in maintaining motor neuron integrity, which

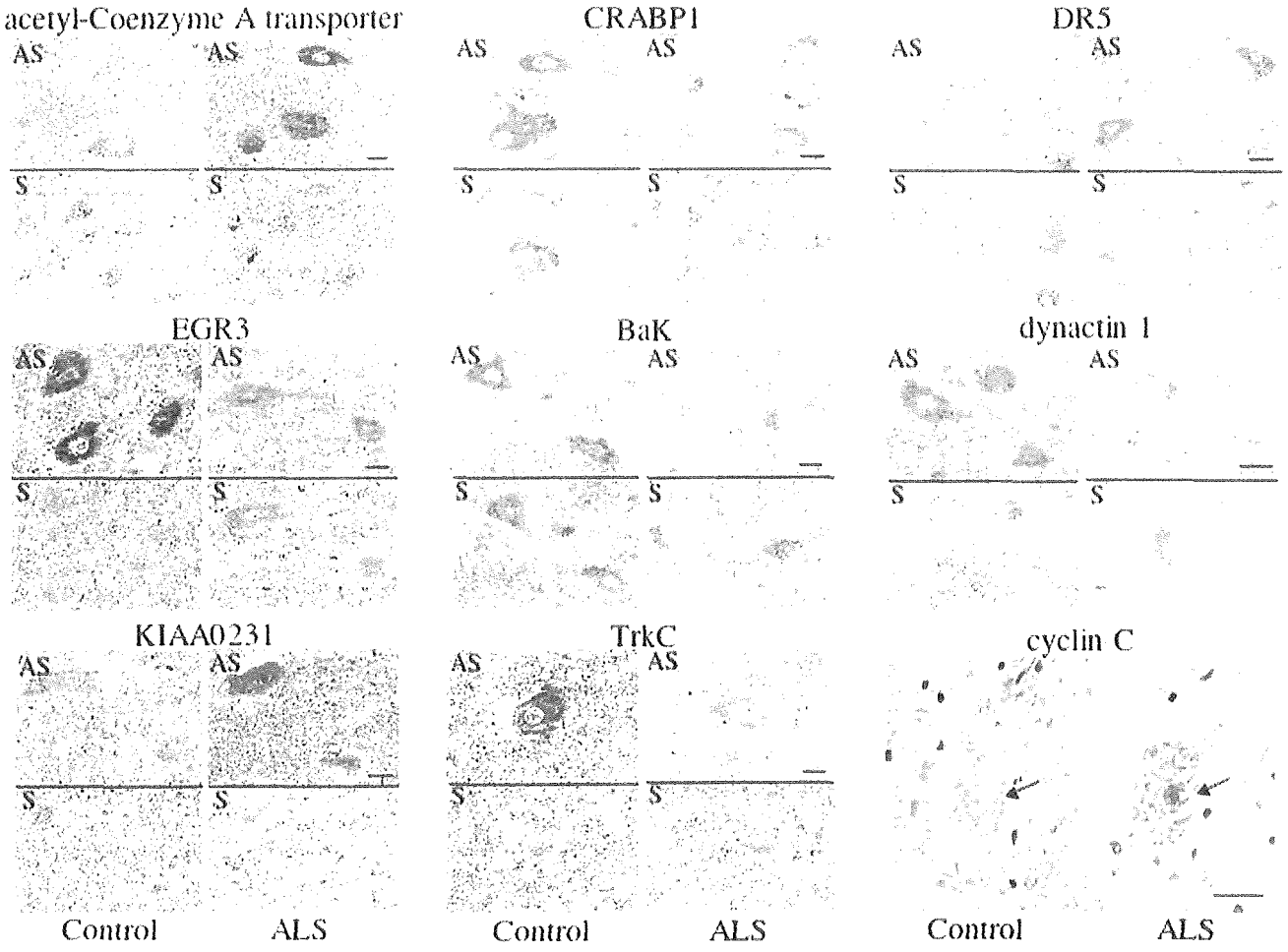


*Fig 4. In situ hybridization and immunohistochemistry of the selected genes. Representative in situ hybridization is shown for acetyl-COENZYMEA transporter, EGR3, KIAA0231, CRABP1, Bak, TrkC, DR5, and dynactin 1. The antisense probe (AS) detects positive signals for the expression of each gene in spinal motor neurons for ALS and/or controls, but the sense probe (S) does not. Lipofuscin granules are seen as yellowish granules. Immunohistochemistry was preformed for cyclin C, and nuclear staining was prominent in ALS motor neurons. Arrows denote the nuclei. Bars = 25μm.*

might be impaired in the neurodegenerative process of ALS. Among the genes related to transcriptional regulation, the number of significantly downregulated genes was twofold greater than that of the upregulated ones in ALS motor neurons. These downregulated transcription-related genes were not restricted to genes regulating neuronal differentiation as neuron-specific cellular properties, but also included genes such as RNA polymerase and transcription factors, which regulate general cellular functions. These observations suggest that downregulation of transcriptional activity may be the reflection of motor neuron dysfunction because of a wide range of impairments of cellular maintenance systems.

Interestingly, the expression of dynactin 1, which recently has been identified as a causative gene for human motor neuron disease,[42] was reduced in ALS motor neurons. Some other motor proteins including the kinesin family responsible for antegrade axonal transport and dyneins for retrograde axonal transport were not changed significantly, but the expression levels of MAPs 1A, 4, and tau were decreased, shown by their classification in SOM1 and SOM6. The impairment of axonal transport is thought to be an early event of motor neuron degeneration, and especially the protein levels of MAPs 1A and tau have been reported to decrease early before the onset of symptoms in mutant SOD1 transgenic mice.[43–45] The upregulation of ubiquitin-specific protease 11 (USP11), listed in Tables 2 and 3, also may be related to microtubule abnormality because the RanGTP-associated protein RanBPM, which is required for correct nucleation of microtubules, is the enzymatic substrate for USP11.[46] The present results imply that retrograde axonal transport, especially that associated with dynactin, might be affected even at the terminal stage of ALS and be crucial for motor neurons, although cytoskeletal proteins are the major functional group in the downregulated genes.

As for the death signals and inflammatory factors, we previously have reported that these genes were significantly upregulated in the spinal cord of mutant SOD1 transgenic mice,[15,17] suggesting that these inflammatory and apoptotic death signals play a crucial role in concert with motor neuron degeneration and inflammatory cellular reactions, including microglial activation.[7,47] However, in sporadic ALS spinal cords, the expression profiles of inflammation- and death signal–related genes are somewhat different from those in the Tg mouse model. Death receptor 5 (TNF receptor 10b, TNFR10b), TNF receptor–associated factor 6 (TRAF 6), interleukin-1 receptor antagonist, and ephrin A1 were overexpressed in ALS motor neurons, whereas the expression levels of the respective ligands or inducers, TNF-α, TNF superfamily member 10 (TRAIL) and IL-1β, were not markedly changed in either motor neurons or ventral horn homogenates. Because TNF-α was prominently upregulated in the Tg mouse spinal cords,[17] its almost unchanged expression level in sporadic ALS was a surprising observation. Many other inflammation-related genes were also not significantly upregulated in human ALS spinal cords, in contrast with the findings in animal models. Far less invasion and activation of microglia, a major source of TNF-α, IL-1β, and many other inflammatory factors, were seen in human ALS spinal cords at the terminal autopsy stage as compared with those of Tg mice,[48] which could explain these differences.

Genes related to apoptotic pathways, caspase-1, -3, -9, caspase, and RIP adaptor with death domain (CRADD), were upregulated in ALS motor neurons in SOM analysis (SOM24 and SOM25), and an antiapoptotic factor, NF-κB, was markedly upregulated. Although Bax, a proapoptotic Bcl-2 family member, has been reported to increase in ALS motor neurons,[49,50] and another member, Bak, was underexpressed in this study, the expression of Bcl-2 and Bcl-xL, antiapoptotic Bcl-2 family members was not significantly altered in motor neurons, possibly suggesting that Bcl-2 family members are not primarily involved in motor neuron degeneration in sporadic ALS. Cyclin A1 and C were upregulated (SOM25) and cyclin E was downregulated (SOM1) in ALS motor neurons. These cell cycle regulators are specific to G1/S phase transition, and upregulation of these cyclins enhances arrest in G1/S phase, preventing entry into S phase. Our finding on cyclin expression support the recently reported view that G1/S phase is aberrantly activated in ALS motor neurons, eventually inducing motor neuron death.[51] The subcellular localization of cyclin C in the nucleus may trigger cell death signaling mechanisms. These factors related to the cell death signaling pathway, TNFR, TRAF6, CRADD, caspases, cyclins, Bak, and NF-κB may be involved in the motor neuron degeneration process in sporadic ALS, although we cannot simply state that an apoptotic process is present in ALS motor neurons, as has been suggested by many histological analyses.[6] Becausse neuronal cell degeneration and the eventual neuronal cell death process are the results of interactions of complex pathways involving many factors and signaling molecules, we need to further elucidate the pathophysiological significance of these factors with altered expression levels in ALS motor neurons.

Microarray analysis on the laser-captured motor neurons provided us with significant information about motor neuron degeneration and dysfunction in sporadic ALS patients. Such information cannot be obtained by whole spinal cord tissue microarray assay,[52] as discussed above. Although this study was performed on postmortem patients' tissues, the remaining individual motor neurons would express ongoing or even early molecular events in the neurodegeneration process, because motor neurons in the remaining motor neuron population randomly enter into the degeneration process among up to the terminal stage in ALS.[53] We need to study larger numbers of ALS patients, and to understand the pathophysiological roles of candidate genes identified by the combined methodology of DNA microarray analysis and LCM, compared with other neurodegeneration processes. This methodology provides crucial clues about candidate genes whose related products might hamper the disease process of ALS.

This work was supported by a Center of Excellence grant from the Ministry of Education, Culture, Sports, Science and Technology of Japan, and grants from the Ministry of Health, Labor and Welfare of Japan.

## References

1. Ince PG, Lowe J, Shaw PJ. Amyotrophic lateral sclerosis: current issues in classification, pathogenesis and molecular pathology. Neuropathol Appl Neurobiol 1998;24:104–117.
2. Bunina TL. On intracellular inclusions in familial amyotrophic lateral sclerosis. Korsakov J Neuropath Psychiat 1962;62: 1293–1296.
3. Okamoto K, Hirai S, Amari M, et al. Bunina bodies in amyotrophic lateral sclerosi immunostained with rabbit anti-cystatin C serum. Neurosci Lett 1993;162:125–128.
4. Cleveland DW, Rothstein JD. From Charcot to Lou Gehrig: deciphering selective motor neuron death in ALS. Nat Rev Neurosci 2001;2:806–819.
5. Bergeron C. Oxidative stress: its role in the pathogenesis of amyotrophic lateral sclerosis. J Neurol Sci 1995;129(suppl): 81–84.
6. Sathasivam S, Ince PG, Shaw PJ. Apoptosis in amyotrophic lateral sclerosis: a review of the evidence. Neuropathol Appl Neurobiol 2001;27:257–274.
7. Hand CK, Rouleau GA. Familial amyotrophic lateral sclerosis. Muscle Nerve 2002;25:135–159.
8. Ishigaki S, Liang Y, Yamamoto M, et al. X-Linked inhibitor of apoptosis protein is involved in mutant SOD1-mediated neuronal degeneration. J Neurochem 2002;82:576–584.

9. Kawahara Y, Ito K, Sun H, et al. Glutamate receptors: RNA editing and death of motor neurons. Nature 2004;427:801.
10. Niwa J, Ishigaki S, Hishikawa N, et al. Dorfin ubiquitylates mutant SOD1 and prevents mutant SOD1-mediated neurotoxicity. J Biol Chem 2002;277:36793–36798.
11. Hishikawa N, Niwa J, Doyu M, et al. Dorfin localizes to the ubiquitylated inclusions in Parkinson's disease, dementia with Lewy bodies, multiple system atrophy, and amyotrophic lateral sclerosis. Am J Pathol 2003;163:609–619.
12. Luo J, Isaacs WB, Trent JM, Duggan DJ. Looking beyond morphology: cancer gene expression profiling using DNA microarrays. Cancer Invest 2003;21:937–949.
13. Alizadeh AA, Ross DT, Perou CM, van de Rijn M. Towards a novel classification of human malignancies based on gene expression patterns. J Pathol 2001;195:41–52.
14. Luo L, Salunga RC, Guo H, et al. Gene expression profiles of laser-captured adjacent neuronal subtypes. Nat Med 1999;5: 117–122.
15. Ando Y, Liang Y, Ishigaki S, et al. Caspase-1 and -3 mRNAs are differentially upregulated in motor neurons and glial cells in mutant SOD1 transgenic mouse spinal cord: a study using laser microdissection and real-time RT-PCR. Neurochem Res 2003; 28:839–846.
16. Ginsberg SD, Hemby SE, Lee VM, et al. Expression profile of transcripts in Alzheimer's disease tangle-bearing CA1 neurons. Ann Neurol 2000;48:77–87.
17. Yoshihara T, Ishigaki S, Yamamoto M, et al. Differential expression of inflammation- and apoptosis-related genes in spinal cords of a mutant SOD1 transgenic mouse model of familial amyotrophic lateral sclerosis. J Neurochem 2002;80:158–167.
18. Kamme F, Salunga R, Yu J, et al. Single-cell microarray analysis in hippocampus CA1: demonstration and validation of cellular heterogeneity. J Neurosci 2003;23:3607–3615.
19. Terao S, Sobue G, Hashizume Y, et al. Disease-specific patterns of neuronal loss in the spinal ventral horn in amyotrophic lateral sclerosis, multiple system atrophy and X-linked recessive bulbospinal neuronopathy, with special reference to the loss of small neurons in the intermediate zone. J Neurol 1994;241: 196–203.
20. Sobue G, Hashizume Y, Yasuda T, et al. Phosphorylated high molecular weight neurofilament protein in lower motor neurons in amyotrophic lateral sclerosis and other neurodegenerative diseases involving ventral horn cells. Acta Neuropathol (Berl) 1990;79:402–408.
21. Bohm M, Wieland I, Schutze K, Rubben H. Microbeam MOMeNT: non-contact laser microdissection of membrane-mounted native tissue. Am J Pathol 1997;151:63–67.
22. Watanabe H, Tanaka F, Doyu M, et al. Differential somatic CAG repeat instability in variable brain cell lineage in dentatorubral pallidoluysian atrophy (DRPLA): a laser-captured microdissection (LCM)-based analysis. Hum Genet 2000;107: 452–457.
23. Schutze K, Lahr G. Identification of expressed genes by laser-mediated manipulation of single cells. Nat Biotechnol 1998;16: 737–742.
24. Wang J, Delabie J, Aasheim H, et al. Clustering of the SOM easily reveals distinct gene expression patterns: results of a reanalysis of lymphoma study. BMC Bioinformatics 2002;3: 36–44.
25. Ross ME, Zhou X, Song G, et al. Classification of pediatric acute lymphoblastic leukemia by gene expression profiling. Blood 2003;102:2951–2959.
26. Malaspina A, Kaushik N, de Belleroche J. Differential expression of 14 genes in amyotrophic lateral sclerosis spinal cord detected using gridded cDNA arrays. J Neurochem 2001;77: 132–145.
27. Dangond F, Hwang D, Camelo S, et al. The molecular signature of late-stage human ALS revelated by expression profiling of post-mortem spinal cord gray matter. Physiol Genomics 2004;16:229–239.
28. Kanamori A, Nakayama J, Fukuda MN, et al. Expression cloning and characterization of a cDNA encoding a novel membrane protein required for the formation of *O*-acetylated ganglioside: a putative acetyl-CoA transporter. Pro Natl Acad Sci USA 1997;94:2897–2902.
29. Malisan F, Franchi L, Tomassini B, et al. Acetylation suppresses the proapoptotic activity of GD3 ganglioside. J Exp Med 2002; 196:1535–1541.
30. Rapport MM, Donnenfeld H, Brunner W, et al. Ganglioside patterns in amyotrophic lateral sclerosis brain regions. Ann Neuol 1985;18:60–67.
31. Chen HH, Tourtellotte WG, Frank E. Muscle spindle-derived neurotrophin 3 regulates synaptic connectivity between muscle sensory and motor neurons. J Neurosci 2002;22:3512–3519.
32. Mears SC, Frank E. Formation of specific monosynaptic connections between muscle spindle afferents and motoneurons in the mouse. J Neurosci 1997;17:3138–3135.
33. Yamamoto M, Sobue G, Yamamoto K, et al. Expression of glial cell line-derived neurotrophic factor mRNA in the spinal cord and muscle in amyotrophic lateral sclerosis. Neurosci Lett 1996; 204:117–120.
34. Zhou H, Muramatsu T, Halfter W, et al. A role of midkine in the development of the neuromuscular junction. Mol Cell Neurosci 1997;10:56–70.
35. Oosthuyse B, Moons L, Storkebaum E, et al. Deletion of the hypoxia-response element in the vascular endothelial growth factor promoter causes motor neuron degeneration. Nat Genet 2001;28:131–138.
36. Lambrechts D, Storkebaum E, Morimoto M, et al. VEGF is a modifier of amyotrophic lateral sclerosis in mice and humans and protects motoneurons against ischemic death. Nat Genet 2003;34:383–394.
37. Gros-Louis F, Laurent S, Lopes AA, et al. Absence of mutations in the hypoxia response element of VEGF in ALS. Muscle Nerve 2003;28:774–775.
38. Kawahara Y, Ito K, Sun H, et al. Low editing efficiency of GluR2 mRNA is associated with a low relative abundance of ADAR2 mRNA in white matter of normal human brain. Eur J Neurosci 2003;18:23–33.
39. Venter JC, Adams MD, Myers EW, et al. The sequence of the human genome. Science 2001;291:1304–1351.
40. Colbert MC, Rubin WW, Linney E, LaMantia AS. Retinoid signaling and the generation of cellular diversity in the embryonic mouse spinal cord. Dev Dyn 1995;204:1–12.
41. Sakakibara S, Okano H. Expression of neural RNA-binding proteins in the postnatal CNS: implications of their roles in neuronal and glial cell development. J Neurosci 1997;17: 8300–8312.
42. Puls I, Jonnakuty C, LaMonte BH, et al. Mutant dynactin in motor neuron disease. Nat Genet 2003;33:455–456.
43. Williamson TL, Cleveland DW. Slowing of axonal transport is a very early event in the toxicity of ALS-linked SOD1 mutants to motor neurons. Nat Neurosci 1999;2:50–56.
44. Zhang B, Tu P, Abtahian F, et al. Neurofilaments and orthograde transport are reduced in ventral root axons of transgenic mice that express human SOD1 with a G93A mutation. J Cell Biol 1997;139:1307–1315.
45. Farah CA, Nguyen MD, Julien JP, Leclerc N. Altered levels and distribution of microtuble-associated protein before disease onset in a mouse model of amyotrophic lateral sclerosis. J Neurochem 2003;84:77–86.

46. Ideguchi H, Ueda A, Tanaka M, et al. Structural and functional characterization of the USP11 deubiquitinating enzyme, which interacts with the RanGTP-associated protein RanBPM. Biochem J 2002;367:87–95.
47. Hensley K, Floyd RA, Gordon B, et al. Temporal patterns of cytokines and apoptosis-related gene expression in spinal cords of the G93A-SOD1 mouse model of amyotrophic lateral sclerosis. J Neurochem 2002;82:365–374.
48. Hall ED, Oostveen JA, Gurney ME. Relationship of microglial and astrocytic activation to disease onset and progression in a transgenic model of familial ALS. Glia 1998;23:249–256.
49. Mu X, He J, Anderson DW, et al. Altered expression of bcl-2 and bax mRNA in amyotrophic lateral sclerosis spinal cord motor neurons. Ann Neurol 1996;40:379–386.
50. Ekegren T, Grundstrom E, Lindholm D, Aquilonius SM. Up-regulation of Bax protein and increased DNA degradation in ALS spinal cord motor neurons. Acta Neurol Scand 1999;100: 317–321.
51. Ranganathan S, Bowser R. Alterations in G(1) to S phase cell-cycle regulators during amyotrophic lateral sclerosis. Am J Pathol 2003;162:823–835.
52. Malaspina A, de Belleroche J. Spinal cord molecular profiling provides a better understanding of amyotrophic lateral sclerosis pathogenesis. Brain Res Brain Res Rev 2004;45:213–229.
53. Sobue G, Sahashi K, Takahashi A, et al. Degenerating compartment and functioning compartment of motor neurons in ALS: possible process of motor neuron loss. Neurology 1983;33: 654–657.

Available online at www.sciencedirect.com

SCIENCE DIRECT®

Developmental Biology 275 (2004) 124–142

DEVELOPMENTAL BIOLOGY

www.elsevier.com/locate/ydbio

# Retinoic-acid-concentration-dependent acquisition of neural cell identity during in vitro differentiation of mouse embryonic stem cells

Yohei Okada[a,b,c], Takuya Shimazaki[a,c], Gen Sobue[b], Hideyuki Okano[a,c,*]

[a]*Department of Physiology, Keio University School of Medicine, Shinjuku-ku, Tokyo 160-8582, Japan*
[b]*Department of Neurology, Nagoya University Graduate School of Medicine, Showa-ku, Nagoya 466-8550, Japan*
[c]*Core Research for Evolutional Science and Technology (CREST), Japan Science and Technology Agency, Kawaguchi, Saitama 332-0012, Japan*

Received for publication 11 February 2004, revised 19 July 2004, accepted 21 July 2004
Available online 8 September 2004

**Abstract**

Retinoic acid (RA) is one of the most important morphogens, and its embryonic distribution correlates with neural differentiation and positional specification in the developing central nervous system. To investigate the concentration-dependent effects of RA on neural differentiation of mouse embryonic stem cells (ES cells), we investigated the precise expression profiles of neural and regional specific genes by ES cells aggregated into embryoid bodies (EBs) exposed to various concentrations of RA or the BMP antagonist Noggin. RA promoted both neural differentiation and caudalization in a concentration-dependent manner, and the concentration of RA was found to regulate dorso-ventral identity, i.e., higher concentrations of RA induced a dorsal phenotype, and lower concentrations of RA induced a more ventral phenotype. The induction of the more ventral phenotype was due to the higher expression level of the N-terminus of sonic hedgehog protein (Shh-N) when treated with low concentration RA, as it was abrogated by an inhibitor of Shh signaling, cyclopamine. These findings suggest that the concentration of RA strictly and simultaneously regulates the neuralization and positional specification during differentiation of mouse ES cells and that it may be possible to use it to establish a strategy for controlling the identity of ES-cell-derived neural cells.


*Keywords:* Embryonic stem cells; Neural differentiation; Retinoic acid; Sonic hedgehog; N-terminus of Sonic hedgehog; Positional identity; Motor neuron; Morphogen

## Introduction

Embryonic stem cells (ES cells) are clonal cell lines derived from the inner cell mass (ICM) of developing blastocysts and under appropriate conditions are capable of proliferating extensively and generating various cell types derived from the three primary germ layers of the embryo in vitro. This pluripotency of ES cells provides a powerful in vitro model for investigating the mechanisms that control differentiation in early embryonic development. The basic strategy for in vitro differentiation usually adopted is to induce cell aggregation into so-called embryoid bodies (EBs) through suspension culture in nonadhesive dishes or hanging drops. Different inducing conditions during EB formation can drastically affect the proportions of the various cell types that differentiate in EBs. For example, exposure to high-concentration RA strongly drives neural induction, whereas low-concentration RA induces cardiomyocyte differentiation (Rohwedel et al., 1999). Because neural cells represent only a small percentage of cells in EBs cultured in the presence of fetal bovine serum (FBS) and the absence of an exogenous inducer, efficient generation of neural cells requires an additional inductive stimulus or other differentiation method.

There are two major strategies for generating neural cells from mouse ES cells: EB formation and serum-free direct induction. The former includes treatment with high-concentration RA (Bain et al., 1995; Fraichard et al., 1995; Strubing et al., 1995), which has been shown to promote

* Corresponding author. Department of Physiology, Keio University, School of Medicine, 35 Shinanomachi, Shinjuku-ku, Tokyo 160-8582, Japan. Fax: +81 3 3357 5445.
*E-mail address:* hidokano@sc.itc.keio.ac.jp (H. Okano).

0012-1606/$ - see front matter © 2004 Elsevier Inc. All rights reserved.
doi:10.1016/j.ydbio.2004.07.038

neural gene expression and repress mesodermal gene expression (Bain et al., 1996), and serum-free culture after EB formation, which enables selection of neural cells (Okabe et al., 1996). Direct induction methods consist of a co-culture system with stromal cell line PA6 as a neural inducer that has been found to have stromal-cell-derived inducing activity (SDIA) (Kawasaki et al., 2000), a low-cell-density neural stem cell (NSC) culture (neurosphere culture) with growth factors (Tropepe et al., 2001), and an adherent monolayer culture method (Ying et al., 2003).

Sequences of events leading to lineage commitment similar to those in vivo are often observed with all of these culture strategies, and, for example, exposure to Noggin or other manipulations that inhibit bone morphogenetic protein (BMPs) signaling, which blocks neural differentiation in the early development, facilitates neural differentiation of ES cells also in vitro (Finley et al., 1999; Gratsch and O'Shea, 2002; Kawasaki et al., 2000; Tropepe et al., 2001).

During the development of the mammalian central nervous system (CNS), the differentiation properties of neural stem cells (NSCs) vary depending on the stage at which they are generated (temporal identity) and their location (positional identity). These properties define the induction and sequential rounds of neurogenesis and gliogenesis, which seem to be regulated by both intrinsic and extrinsic factors, and limit their plasticity (Temple, 2001). Depending on their location, their differentiation is usually regulated by secreting signals that modulate the rostro-caudal or dorso-ventral axis of the body and by regional cues that define the borders of each CNS segment (Hitoshi et al., 2002; Temple, 2001). In view of these characteristics of NSCs, the temporal and positional identity of NSCs derived from ES cells may be controlled in vitro by the conditions under which they differentiate, the same as specification in vivo. Indeed, much interest has been focused on the generation of specific types of neurons or neural progenitors from ES cells by producing these identities with inductive signals, such as fibroblast growth factor (FGF) 8 and Shh, or with SDIA for dopaminergic neurons (Kawasaki et al., 2000, 2002; Kim et al., 2002; Lee et al., 2000; Ying et al., 2003), RA and Shh for motor neurons (Renoncourt et al., 1998; Wichterle et al., 2002), and a combination of SDIA and BMPs for dorsal and neural-crest-derived cells (Mizuseki et al., 2003).

RA is well known as the biologically active form of vitamin A and has been shown to play an important role during embryogenesis (Ross et al., 2000). RA influences neural development in the early stage of CNS development and is required to establish patterned territories of cell groups, which, for example, has been observed in rostro-caudal axis formation, according to the distribution of RA in experiments on *Xenopus* (Blumberg et al., 1997; Sive et al., 1990) and mice (Kessel, 1992; Kessel and Gruss, 1991; Marshall et al., 1992). For these reasons, RA has been thought to be one of the most important extrinsic inductive signals that can be used for neural differentiation of mouse ES cells in vitro. However, its overall effects have yet to be clearly identified, and precise analysis of alterations of gene expression caused by RA treatment should be useful for establishing proper culture protocols for the differentiation of ES cells. In the present study, we demonstrated that RA promotes neural differentiation and caudalization in a concentration-dependent manner, and that the concentration of RA affects dorso-ventral positional identity, by determining the precise gene expression profiles during differentiation of ES cells.

## Materials and methods

### *ES cell culture*

Mouse ES cells (EB3) were maintained and used for induction. ES cells were grown on gelatin-coated (0.1%) tissue culture dishes in standard ES-cell culture medium containing GMEM (Sigma G6148) supplemented with 10% FBS, glutamine (2 mM), nonessential amino acids (0.1 mM), sodium pyruvate (1 mM), 2-mercaptoethanol (2-ME) (0.1 mM), sodium bicarbonate (3 mM), HEPES (5 mM), and mLIF. EB3 is a subline derived from E14tg2a ES cells (Hooper et al., 1987) that was generated by targeted integration of Oct3/4-IRES-BSD-pA vector (Niwa et al., 2000) into the *Oct3/4* allele, and it was maintained in the medium containing 10 μg/ml blasticidin S to eliminate differentiated ES cells.

### *Differentiation of ES cells*

For embryoid body (EB) formation, ES cells were detached and dissociated into single cells with 0.25% trypsin–EDTA and then plated onto a bacteriological dish (Kord-Valmark™) in 10 ml of αMEM (Gibco 11900-024) supplemented with 10% FBS, sodium bicarbonate (3 mM), and 0.1 mM 2-ME (EB medium) at a density of $5 \times 10^4$ cells/ml. On day 2, various concentrations of all-*trans*-retinoic acid (RA: Sigma R 2625) were added to the culture medium (2−/4+ protocol). RA was reconstituted with 100% ethanol to prepare a stock solution. It should be noted that the effective RA concentrations at which ES cells grow into EBs may be considerably higher than those indicated in the text, because FBS contains significant levels of RA. Furthermore, cells within EBs may produce endogenous RA, possibly as a secondary effect of the initially added RA. However, we used conditions in which FBS did not contain exogenous RA as a negative control (stated control in the figures), and evaluated the results in terms of relative concentrations of RA. Recombinant mouse Sonic Hedgehog (Shh) protein (amino-teminal peptide) (Shh-N; R&D Systems Inc., 461-SH) and cyclopamine (0.1 μM, 1 μM, Toronto Research Chemicals Inc., C988400) were also added on day 2 of the experiment. For Noggin treatment, 10% (v/v) culture supernatant of Cos7

cells transfected with *Xenopus* Noggin/MC BOS (a gift of Y. Takahashi) (Kohyama et al., 2001; Tonegawa and Takahashi, 1998) (xNoggin conditioned medium) was added.

EBs were collected at day 6 of culture and allowed to settle to the bottom of the tube for a few minutes. The cells were then washed once with PBS and incubated with 0.25% trypsin–EDTA for 5 min at 37°C. The enzymatic reaction was quenched by addition of an equal volume of EB medium, and the cells were dissociated with a transfer pipette by triturating 30 times. The cells were then washed twice with serum-free αMEM and resuspended in Media hormone mix (MHM) medium, which contains DMEM/F-12 (1:1) (Gibco 12100-046, 21700-075), glucose (0.6%), glutamine (2 mM), sodium bicarbonate (3 mM), HEPES (5 mM), insulin (25 μg/ml), transferrin (100 μg/ml), progesterone (20 nM), sodium selenate (30 ng), and putrescine (60 nM) (all from Sigma except for DMEM/F-12) as described previously (Shimazaki et al., 2001). The dissociated EBs were plated on poly-L-ornithine/fibronectin-coated 10-mm cover glasses (Matsunami) at a cell density of $1.6 \times 10^5$ cells/0.75 $cm^2$ on a 48-well culture plate (Coaster) and allowed to differentiate for 24 h.

To clarify the effects of RA added at different points in time or of exposure for different periods of culture, ES cells were differentiated into EBs based on 2−/2+/2−, 2−/2+/2+ and 4−/4+ protocols (Suppl. Fig. 1). In the 2−/2+/2− and 2−/2+/2+ protocol, various concentrations of RA were added on day 2, and on day 4 the culture medium was replaced with freshly prepared medium containing the same concentrations of RA (2−/2+/2+ protocol) or no RA (2−/2+/2− protocol). In the 4−/4+ protocol, various concentrations of RA were added to the culture medium on day 4. Total RNA was isolated at day 0, 2, 4, 6, and 8 and processed for RT-PCR analysis.

*Immunocytochemistry*

Dissociated EBs were cultured for 24 h and fixed with 4% paraformaldehyde for 20 min at room temperature. The cells were rinsed with PBS twice and pretreated with PBS containing 0.3% Triton -X100 for 5 min at room temperature. After blocking in TNB buffer (Provided by NEN™ Life Science Products, Inc.) for 1 h at room temperature, the cells were incubated at 4°C overnight with the following antibodies: anti-Nestin (Rat-401, mouse IgG, 1:200), anti-Islet-1/2 (40.2D6, mouse IgG, 1:500), anti-Lim3 (67.4E12, mouse IgG, 1:1000), anti-HB9 (81.5C10, mouse IgG, 1:100), anti-Otx1 (Otx-5F5, mouse IgG, 1:500000), anti-Nkx2.2 (74.5A5, mouse IgG, 1:5000), anti-Pax7 (mouse IgG, 1:5000) (Developmental Studies of Hybridoma Bank: DSHB), anti-βIII-tubulin (mouse IgG, 1:1000, Sigma T8660), anti-Olig2 (rabbit IgG, 1:30000) (Mizuguchi et al., 2001; Takebayashi et al., 2000), anti-Phox2b (rabbit IgG, 1:25000) (Pattyn et al., 1997), anti-Nkx6.1 (Ab174.3, rabbit IgG., 1:200000) (Jensen et al., 1996), anti-Group B1 Sox [Sox1/(2)/3] (rabbit IgG, 1:10000) (Tanaka et al., unpublished). Anti-Group B1 Sox [Sox1/(2)/3] antibody is weakly reactive with Sox2, which is expressed not only by the neural primordium but by undifferentiated ES cells, and with Sox1 and Sox3 (with preference for Sox1 and Sox3 over Sox2). However, as all Group B1 Sox genes are expressed in neural primordium (Wood and Episkopou, 1999), we used this antibody to detect neural progenitors, by determining the immunostaining conditions under which undifferentiated ES cells, which were used as a negative control, did not stain (data not shown). Antigen retrieval was accomplished by incubating the samples in the boiled PBS for 10 min for anti-Isl-1/2 and anti-Lim3, in boiled Target Retrieval Solution (DAKO) for 10 min for anti-Nkx2.2, or in 1 N HCl at 30°C for 15 min for anti-Pax7. After washing with PBS three times, the cells were incubated for 1 h at room temperature with secondary antibodies conjugated with Alexa 488 or Alexa 568 (Molecular Probes). For anti-Islet1/2, anti-Lim3, anti-HB9, anti-Olig2, anti-Phox2b, anti-Otx1, anti-Nkx2.2, anti-Pax7, and anti-Nkx6.1 staining, we used biotinylated secondary antibodies (Jackson Immunoresearch Laboratory, Inc.) after exposure to 1% $H_2O_2$ for 15 min at room temperature to inactivate endogenous peroxidase. The signals were then enhanced with streptavidin-HRP (SA-HRP), followed by TSA™ Fluorescein System (NEN™ Life Science Products, Inc.). After washing with PBS, the samples were mounted on slides and examined with a universal fluorescence microscope (Axiophot 2, Carl Zeiss) and a confocal laser scanning microscope (LSM510, Carl Zeiss). The nuclei of all samples were stained with hoechst33342 (1 μg/ml, Sigma B2261). For statistical analysis, at least 200 cells per cover glass were examined, and the numbers of cells that had immunoreacted with each antibody were counted and expressed as a percentage of the total number of cells whose nuclei stained with hoechst33342. The *P* values for statistical significance (*t* test) are stated in the figure legends.

*Western blot analysis*

Western blot analysis was performed by the previously established method. A 20 μg protein sample of a total cell extract was run on 7.5–15% SDS-PAGE, transferred to nitrocellulose, and probed with each antibody. The blot was probed with the following antibodies: anti-Nestin (Rat-401, mouse IgG, Developmental Studies of Hybridoma Bank: DSHB), anti-βIII-tubulin (mouse IgG, Sigma T8660), anti-Glial Fibrillary Acidic Protein (GFAP) (rabbit IgG, DAKO Z0334), anti-CNPase (mouse IgG, Sigma C5922), and anti-Shh N-terminal fragment (goat IgG, Santa Cruz sc-1194). Signals were detected with HRP-conjugated secondary antibodies (Jackson Immunoresearch Laboratory, Inc.) by using an ECL kit (Amersham Biosciences). Quantitative analysis was performed with Scion Image (Scion Corpo-

ration). The amounts of proteins loaded in each slot were normalized to those of α-tubulin.

*RNA isolation and RT-PCR*

RT-PCR analysis of at least two independent cultures was performed in most of the experiments, and were similar results obtained. Total RNA was isolated with Trizol reagent (Invitrogen™ 15596-018) and DNase I treatment, or by the RNeasy Mini Kit (Qiagen). Total RNA (1–3 μg) was used to synthesize cDNA with 500 ng oligo-d(T)$_{12-18}$ primers. The cDNA synthesis was performed at 42°C for 50 min in a final volume of 20 μl according to the manufacturer's instructions for Superscript II RNase H$^-$ reverse transcriptase (Invitrogen™). To analyze relative expression of different mRNAs, the amount of cDNA was normalized based on the signals from ubiquitously expressed *β-actin* mRNA. The PCR was carried out by using a KOD Plus kit (Toyobo) according to the manufacturer's standard protocol in a final volume of 25 μl. Primer sequences and PCR cycling conditions will be provided upon request. To provide negative controls and exclude contamination by genomic DNA, the reverse transcriptase was omitted in the cDNA synthesis step, and the samples were subjected to the PCR reaction in the same manner with primer sets for *β-actin*, and are indicated at the bottom of each figure as RT(−). PCR products were electrophoresed in agarose gel, and bands were visualized with ethidium bromide under UV light. The identity of the PCR products was confirmed by sequencing.

## Results

*Differentiation potential of mouse ES cells regulated by RA*

RA has been shown to be one of the most important extrinsic morphogens and precisely modulates the differentiation properties of ES cells into various cell types, including neural cells, skeletal muscle cells, adipocytes, cardiomyocytes, and vascular smooth muscle cells, in an incubation-time- and concentration-dependent manner (Rohwedel et al., 1999). To examine the concentration-dependent effects of RA on the differentiation of ES cells, we first differentiated ES cells by inducing the formation of EBs in the presence of various concentrations of RA. We also used Noggin, a secreted protein that plays a role in neural induction by inhibiting BMP-signaling (Finley et al., 1999; Gratsch and O'Shea, 2002; Kawasaki et al., 2000; Smith and Harland, 1992; Tropepe et al., 2001; Zimmerman et al., 1996), to investigate RA-independent neural differentiation. ES cells were plated onto bacteriological dishes and had been cultured for 6 days in medium containing various concentrations of RA (added on day 2) or xNoggin conditioned medium (Fig. 1), and they were analyzed by RT-PCR for markers of the three primary germ layers

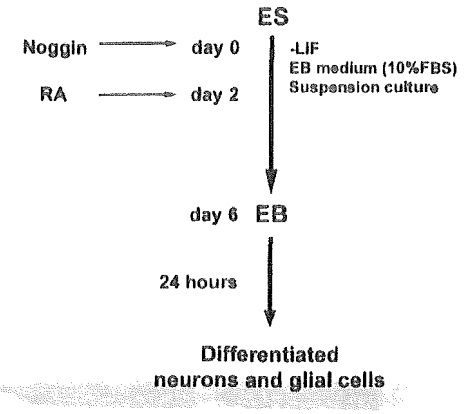


Fig. 1. Experimental protocol for differentiation of ES cells with retinoic acid (RA) or xNoggin conditioned medium. ES cells were cultured in the bacteriological dish for 6 days and formed embryoid bodies (EBs). Various concentrations of RA were added on day 2 of EB formation. Then, EBs were dissociated and differentiated on poly-L-ornithine/fibronectin-coated cover glasses.

(Fig. 2). On day2, *oct3/4*, which is a marker for undifferentiated ES cells, was expressed by both control and Noggin-treated EBs. From day 4 of EB formation onward, *oct3/4* expression was gradually down-regulated by RA in a concentration-dependent manner and in a culture period-dependent manner, and it became undetectable on day 6 under all conditions, indicating that most of the ES cells had differentiated by 6 days of EB formation. On day 6, expression of *ck-17 (cytokeratin 17)*, a marker of epidermis (McGowan and Coulombe, 1998), and expression of *ngn2*, which is expressed in neuronal progenitors (Mizuguchi et al., 2001; Novitch et al., 2001; Ross et al., 2003), were enhanced by high-concentration RA treatment (>$10^{-7}$ M; high-RA), and thus ectodermal differentiation was promoted by exposure to high-RA. Expression of *ck-17* mRNA in undifferentiated ES cells, which also expressed *oct3/4* (Fig. 2), was also demonstrated in a previous study (Tropepe et al., 2001). In the control, Noggin, and low-RA-treated EBs, its expression coincided with expression of *oct3/4* at day 4, and was then down-regulated by day 6 along with extinction of *oct3/4*. In the high-RA-treated EBs, on the other hand, expression of *ck-17* mRNA was detected at day 4 and day 6, without expression of *oct3/4*. The expression of *ck-17* in the absence of expression of *oct3/4* can be understood as indicating promotion of epidermal differentiation in EBs treated with high-RA. Mesodermal differentiation, represented by expression of *brachyury*, which is essential for the formation and organization of mesoderm (Herrmann et al., 1990; Wilkinson et al., 1990), and expression of homeobox gene *nkx2.5*, the earliest known marker of cardiac development (Komuro and Izumo, 1993; Lints et al., 1993), were facilitated by low-concentration RA treatment ($10^{-9}$–$10^{-8}$ M; low-RA). Endodermal markers, including *gata4*, expressed in primitive endoderm (Arceci et al., 1993), and *pdx1*, expressed in developing pancreas (Jonsson et al., 1994; Offield et al., 1996), were

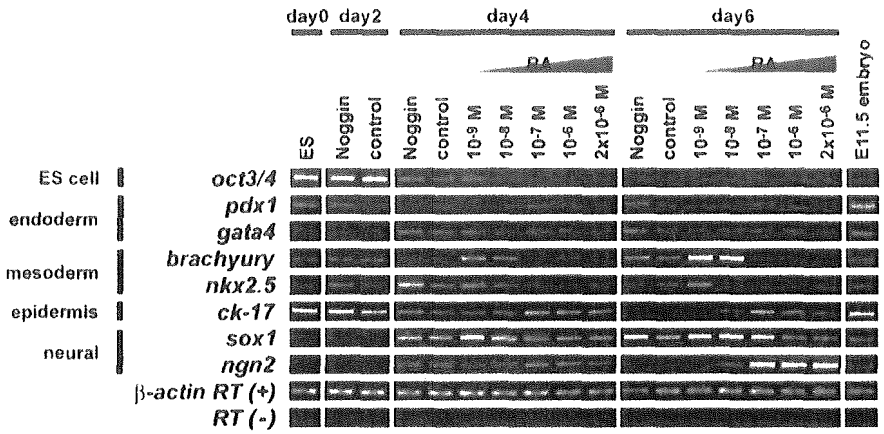


Fig. 2. Expression of markers of the three primary germ layers in EBs exposed to various concentrations of RA. RNA was isolated from ES cells (day 0) and EBs (days 2, 4, 6) and analyzed by RT-PCR for expression of markers of undifferentiated ES cells (*oct3/4*), endoderm differentiation (*pdx1* and *gata4*), mesoderm differentiation (*brachyury* and *nkx2.5*), epidermis differentiation (*ck-17*), and neural differentiation (*sox1* and *ngn2*). To normalize their expression to the amount of cDNA present in the sample, the cDNA for endogenous *β-actin* was amplified.

expressed unstably at low levels, and their levels correlated poorly with the concentrations of RA.

*Neural induction of mouse ES cells by RA*

It has been shown that neural differentiation of ES cells can be promoted by RA, especially by early exposure of EBs to relatively high RA concentrations (Bain et al., 1995, 1996; Fraichard et al., 1995; Gajovic et al., 1997; Renoncourt et al., 1998; Rohwedel et al., 1999; Strubing et al., 1995; Wichterle et al., 2002). However, as the effect of different RA concentrations had never been precisely described, we next investigated how RA promotes neural differentiation. EBs that had been cultured for 6 days were analyzed for differentiation markers of neural cells (progenitors, neurons, and glia) by Western blotting (Figs. 3A, B). Nestin, which is expressed in undifferentiated neural progenitors, was more strongly expressed in EBs treated with low-RA. Expression of βIII-tubulin and GFAP, which are markers of differentiated neurons and astrocytes, respectively, increased in a concentration-dependent manner in EBs exposed to RA (Figs. 3A, B). By contrast, RT-PCR analysis on day 6 showed that expression of *sox1* (a marker of undifferentiated neural cells; Pevny et al., 1998; Wood and Episkopou, 1999) mRNA was higher in EBs treated with low-RA on day 6 (Fig. 2). Expression of CNPase, a marker of oligodendrocytes, was detected only slightly under all of the differentiating conditions, and its expression was not very strongly affected by the concentration of RA (Figs. 3A,B). To better understand the effects of RA on neural differentiation of EBs, we performed immunocytochemistry of markers of various neural lineages (Figs. 3C–E and 5A,B). EBs that had been cultured for 6 days were dissociated and differentiated on poly-L-ornithine/fibronectin-coated cover glasses for 24 h and then processed for immunocytochemistry of markers of undifferentiated neural cells (Nestin, Group B1 Sox, Olig2) and postmitotic neurons (βIII-tubulin). Olig2 is a basic-helix-loop-helix (bHLH) transcription factor that is expressed in most of the ventral neural progenitor cells around the period of neural tube closure (Takebayashi et al., 2000). Treatment of EBs with low-RA ($10^{-8}$ M) induced a 1.6-, 3.0-, and 9.1-fold increase in Nestin-, Group B1 Sox, and Olig2-positive undifferentiated neural progenitors, respectively, over those treated with high-RA ($2 \times 10^{-6}$ M) (Figs. 3C–E). Treatment of EBs with high-RA ($2 \times 10^{-6}$ M) induced very few Nestin-, Group B1 Sox-, and Olig2-positive progenitor cells, and instead induced many βIII-tubulin-positive postmitotic neurons [3.0-fold more than by treatment with low-RA ($10^{-8}$ M)] (Figs. 3C–E and 5A). RT-PCR analysis showed that *olig2* was expressed in EBs treated with high-RA at day 4 and down-regulated by day 6, whereas it was expressed highly on day 6 in EBs treated with low-RA (Fig. 6A). These results indicate that higher concentrations of RA facilitate differentiation of neural progenitors into postmitotic neurons and glia, in contrast to lower concentrations of RA, which preferentially induce undifferentiated neural progenitor cells from ES cells; that is, that RA strongly promotes terminal differentiation of ES-cell-derived neural progenitors in a concentration- and culture-period-dependent manner in addition to its action that promotes neural induction of ES cells.

*ES-cell-derived neural cells acquire positional identity through EB formation*

To investigate how RA regulates the specification of rostro-caudal and dorso-ventral positional identity during EB formation, RT-PCR analysis of regionally specific markers was performed (Carpenter, 2002; Caspary and Anderson, 2003; Helms and Johnson, 2003; Hitoshi et al., 2002; Jessell, 2000; Marquardt and Pfaff, 2001;